Hypergrowth mTORC1 Signals Translationally Activate the ARF Tumor Suppressor Checkpoint

Alexander P. Miceli, Anthony J. Saporita and Jason D. Weber

Updated information and services can be found at:
http://mcb.asm.org/content/32/2/348

These include:

REFERENCES

This article cites 55 articles, 28 of which can be accessed free at: http://mcb.asm.org/content/32/2/348#ref-list-1

CONTENT ALERTS

Receive: RSS Feeds, eTOCs, free email alerts (when new articles cite this article), more»

Hypergrowth mTORC1 Signals Translationally Activate the ARF Tumor Suppressor Checkpoint

Alexander P. Miceli, Anthony J. Saporita, and Jason D. Weber

BRIGHT Institute, Department of Internal Medicine, Division of Molecular Oncology, and Department of Cell Biology and Physiology, Siteman Cancer Center, Washington University School of Medicine, Saint Louis, Missouri, USA

The ARF tumor suppressor is a potent sensor of hyperproliferative cues emanating from oncogenic signaling. ARF responds to these cues by eliciting a cell cycle arrest, effectively abating the tumorigenic potential of these stimuli. Prior reports have demonstrated that oncogenic Ras^{V12} signaling induces ARF through a mechanism mediated by the Dmp1 transcription factor. However, we now show that ARF protein is still induced in response to Ras^{V12} in the absence of *Dmp1* through the enhanced translation of existing *Arf* mRNAs. Here, we report that the progrowth Ras/tuberous sclerosis complex (TSC)/mTORC1 signaling pathway regulates ARF protein expression and triggers ARF-mediated tumor suppression through a novel translational mechanism. Hyperactivation of mTORC1 through *Tsc1* loss resulted in a significant increase in ARF expression, activation of the p53 pathway, and a dramatic cell cycle arrest, which were completely reversed upon *Arf* deletion. ARF protein induced from Ras^{V12} in the absence of *Dmp1* repressed anchorage-independent colony formation in soft agar and tumor burden in an allograft model. Taken together, our data demonstrate the ability of the ARF tumor suppressor to respond to hypergrowth stimuli to prevent unwarranted tumor formation.

Regulatory checkpoints are key for maintaining homeostasis in the cell. Transit through the mammalian cell cycle is tightly regulated by a series of essential checkpoints that prevent progression in the presence of hyperproliferative signals or genotoxic insults, such as DNA damage, a stalled replication fork, or improper spindle assembly (7, 9, 22). These and several other regulatory checkpoints are so critical for cellular homeostasis that their loss contributes to the deleterious events that are among the hallmarks of cancer (12).

The ARF tumor suppressor functions as an important checkpoint in the cell, acting as a key sensor of hyperproliferative signals. ARF is one of the two tumor suppressors encoded by the *CDKN2A* (*Ink4a/Arf*) locus (37). ARF functions in both p53-dependent and p53-independent manners (42). *Arf*$^{-/-}$ mice are highly tumor prone, predominantly developing spontaneous fibrosarcoma and lymphoma malignancies (20, 21). Deletion or silencing of the *Ink4a/Arf* locus through hypermethylation of the promoters is extremely common in a multitude of human tumors; among these are numerous examples where ARF function is specifically abrogated independently of p16^{INK4a} (40). These observations underscore the significance of the antitumorigenic functions of ARF and the necessity of cancer cells to evade ARF tumor suppression.

Basal expression of ARF is nearly undetectable. However, ARF protein levels are robustly upregulated in response to excessive proliferative cues, such as those emanating from the Ras^{V12}, Myc, E1A, v-Abl, and E2F oncoproteins (3, 8, 34, 38, 56). Upon induction, ARF binds MDM2, the E3 ligase responsible for targeting p53 for proteasome-mediated degradation (52). ARF's sequestration of MDM2 in the nucleolus allows p53 to accumulate in the nucleoplasm and to activate downstream targets that trigger cell cycle arrest (53).

Cell proliferation and cell growth are intimately linked. As such, proliferative and growth stimuli often invoke cross talk at key signaling networks to properly regulate the timing of cell cycle progression and protein synthesis. A key player in this regulation

is the mammalian target of rapamycin (mTOR) signal transduction pathway (36). mTOR is a conserved serine/threonine kinase that assembles into two major multiprotein-containing complexes, mTORC1 and mTORC2 (57), each of which is reported to serve a unique function in the cell (29). mTORC1 contains Raptor, LST8, Deptor, PRAS40, and mTOR and is critical for regulating protein synthesis; mTORC2 includes Rictor, LST8, Deptor, Protor, Sin1, and mTOR and plays a role in cytoskeletal organization (57). mTOR responds to several upstream stimuli, including growth factors and nutrients. Upstream signaling is propagated through Ras and phosphatidylinositol 3-kinase (PI3K) (41). In addition, the tuberous sclerosis complex (TSC) gene products are critical upstream negative regulators of mTORC1 signal transduction (15); loss of either *Tsc1* or *Tsc2* results in constitutive mTORC1 signaling and increased phosphorylation of S6K1 (ribosomal protein S6 kinase 1) and initiation factor 4E binding protein 1 (4EBP1). This has direct consequences for the protein translation machinery and the downstream gene targets that are regulated by this pathway (14). Mutations among pathway members are common in hamartoma-forming syndromes and a broad spectrum of human cancers (11, 13).

Given ARF's central role in sensing hyperproliferative signals, we hypothesized that ARF might also be sensitive to hypergrowth cues emanating from mTORC1 signaling. In this report, we investigated ARF gene expression and function in response to hyperactivation of the progrowth mTORC1 signal transduction pathway. Importantly, we also interrogated ARF function in the absence of

collaborating signals from the Dmp1 transcription factor, the only known regulator of ARF induction from Ras^{V12}. Ras^{V12} expression in murine embryonic fibroblasts (MEFs) lacking *Dmp1* resulted in increased ARF protein levels, suggesting that (i) Dmp1-mediated transcription of *Arf* is not obligatory for ARF induction and (ii) another pathway downstream of Ras must modulate ARF expression. Using pharmacological and genetic manipulation, we now show that the Ras/TSC/mTORC1 pathway regulates ARF through a novel translational mechanism. Based on our findings, we propose that ARF can respond to hypergrowth signals emanating from a hyperactivated mTORC1 pathway to prevent tumor formation.

MATERIALS AND METHODS

Mice and cell culture. *Tsc1$^{flox/flox}$* mice were a generous gift from Jeffrey Arbeit (Washington University, St. Louis, MO) (23), with permission from David Kwiatkowski (Harvard University, Cambridge, MA). *Tsc1$^{flox/flox}$* and *Arf$^{-/-}$* mice were intercrossed for several generations to generate *Tsc1$^{flox/flox}$; Arf$^{-/-}$* mice. Inbred homozygous female athymic nude mice (*Foxn1^{nu}/Foxn1^{nu}*) were purchased from Jackson Laboratory (Bar Harbor, ME). Nude mice were 5 weeks old at the time of purchase and were housed in our facility until they were approximately 7 weeks of age to acclimate to the new facility before injections were performed. Low-passage (passage 3 [P3] to P5) primary murine embryonic fibroblasts for all described genotypes were established as previously described (21) and maintained in Dulbecco's modified Eagle's medium supplemented with 10% fetal bovine serum, 2 mM glutamine, 0.1 mM nonessential amino acids, 2 μg/ml gentamicin. Etoposide (Sigma, St. Louis, MO) and rapamycin (LC Laboratories, Woburn, MA) were, respectively, used at final concentrations of 50 μM and 100 nM.

Viral production and infections. pBabe-puro-H-Ras^{V12} was a generous gift from Martine Roussel (St. Jude Children's Research Hospital, Memphis, TN). pBabe-HA-ARF (where HA is hemagglutinin), pWZL-GFP-IRES-blast (where GFP is green fluorescent protein and blast is blasticidin), and pWZL-Ras^{V12}-IRES-blast have been previously described (4, 51). Retroviral production was performed as previously described (4, 39). Retroviral helper DNA was kindly provided by Charles Sawyers (University of California Los Angeles, Los Angeles, CA). Collected retrovirus was used to infect MEFs in the presence of 10 μg/ml Polybrene. Infected MEFs were selected in 2 μg/ml puromycin and were harvested for analysis at 5 days postinfection. For the production of lentiviruses encoding short hairpin RNAs, 5×10^5 293T cells were cotransfected using Lipofectamine 2000 (Invitrogen, Carlsbad, CA) with pHCMV.G, CMVΔR8.2, and pLKO.1-puro constructs. Viral supernatants were collected and pooled. Infected MEFs were selected in 2 μg/ml puromycin and were harvested for analysis at 5 days postinfection. High-titer adenoviruses encoding β-galactosidase (Ad5CMVntLacZ [Ad-LacZ]) or Cre recombinase (Ad5CMVCre [Ad-Cre]) were purchased from the Gene Transfer Vector Core, University of Iowa. For adenovirus infections, MEFs were washed with phosphate-buffered saline (PBS), trypsinized, and counted; 7.5×10^5 cells were plated in the presence of LacZ- or Cre-encoding adenovirus for 6 h. Cells were split upon reaching confluence and then harvested for analysis at 9 to 10 days postinfection.

RNAi. pLKO.1-puro constructs obtained from the Genome Center at Washington University were used for RNA interference (RNAi) against *Tsc1*. Sequences for the short hairpin RNAs are 5′-GCCTCGTATGAAG ATGGCTAT-3′ for *Tsc1* (here named siTSC1.2), 5′-GCCAGTGTTTAT GCCCTCTTT-3′ also for *Tsc1* (here named siTSC1.4), 5′-GCGGTTGCC AAGAGGTTCCAT-3′ for the luciferase control, and 5′-CCTAAGGTTA AGTCGCCCTCGCTCGAGGGCGACTTAACCTTAGG-3′ for the scrambled control. pLKO-GFP-shARF has been previously described (1); for the present studies, the GFP marker was replaced by a puromycin resistance cassette subcloned into the BamHI and KpnI sites of pLKO. Lentiviruses were packaged, and MEFs were infected as described above.

For RNAi against *Raptor* and *Rictor*, short hairpin RNA oligonucleotides were purchased from Qiagen (Valencia, CA) and were transduced using the Nucleofector system (Amaxa, Walkersville, MD) according to the manufacturer's instructions. Sequences for the short hairpin RNAs recognizing *Raptor* and *Rictor*, respectively, are 5′-CCGGGTCATGACTTA CCGAGA-3′ and 5′-CAGAAAGATGATTACTGTGAA-3′.

Western blotting. Harvested cells were resuspended and sonicated in radioimmunoprecipitation assay (RIPA) lysis buffer (50 mM Tris-HCl, pH 7.4, 150 mM NaCl, 1% Triton X-100, 0.1% SDS, 0.5% deoxycholic acid) containing protease and phosphatase inhibitors (1 mM phenyl-methylsulfonyl fluoride [PMSF], 0.4 U/ml aprotinin, 10 μg/ml leupeptin, 10 μg/ml pepstatin, 1 mM β-glycerophosphate, 0.1 mM NaF, 0.1 mM NaVO$_4$). Proteins (30 to 80 μg) were separated on 12.5% sodium dodecyl sulfate (SDS)-containing polyacrylamide gels. Separated proteins were transferred onto polyvinylidene difluoride (PVDF) membranes (Millipore, Boston, MA). Membranes were probed with the following antibodies: rabbit anti-Rictor (A300-459), rabbit anti-TSC1 (A300-316), and rabbit anti-glyceraldehyde-3-phosphate dehydrogenase (anti-GAPDHj A300-641) (all from Bethyl Laboratories; Montgomery, TX); rat anti-ARF (ab26696; Abcam, Cambridge, MA); mouse anti-MDM2 (op115; Calbi-ochem/EMD Chemicals, Gibbstown, NJ); mouse antiactin (sc8432), mouse anti-p21 (sc6246), rabbit antinucleophosmin (anti-NPM; sc6013), mouse anti-γ-tubulin (sc17787), and rabbit anti-Ras (sc520) (all from Santa Cruz Biotechnology, Santa Cruz, CA); rabbit anti-p53 (2524), rabbit anti-phospho-extracellular signal-regulated kinase 1 and 2 (anti-phospho-ERK1/2), Thr 202/Tyr 204 (4377), rabbit anti-ERK1/2 (9102), rabbit anti-phospho-S6, Ser 240/244 (2215), mouse anti-S6 (2317), rabbit anti-Raptor (4978), rabbit anti-phospho-4EBP1, Thr37/46 (2855), rabbit anti-YEBP1 (9452), and rabbit anti-p70 S6K1 (9202) (all from Cell Signaling Technologies, Danvers, MA). Secondary horseradish peroxidase-conjugated anti-rabbit, anti-rat, or anti-mouse antibodies (Jackson ImmunoResearch, West Grove, PA) were added, and Amersham ECL Plus (GE Healthcare, Piscataway, NJ) was used to visualize the bands.

Quantitative RT-PCR and endpoint PCR. Total RNA was extracted from cells with a Nucleospin RNAII system (Clontech, Mountain View, CA) according to the manufacturer's instructions. Reverse transcription (RT) reactions were performed using a SuperScript III first-strand synthesis system (Invitrogen, Carlsbad, CA) with an oligo(dT) primer. Real-time PCR was performed on an iCycler apparatus (Bio-Rad, Hercules, CA) using iQ Sybr Green Supermix (Bio-Rad, Hercules, CA). Fold change was calculated using the $\Delta\Delta C_T$ (where C_T is threshold cycle) method (28). To measure *Arf* mRNA, the following primers were used: forward, 5′-GA GTACAGCAGCGGGAGCAT-3′; reverse, 5′-ATCATCATCACCTGGTC CAGGATTCC-3′. To measure *Gapdh* mRNA, the following primers were used: forward, 5′-GCTGGGGCTCACCTGAAGGG-3′; reverse: 5′-GGA TGACCTTGCCCACAGCC-3′.

To assess the presence of *Dmp1* mRNA in MEF samples, total RNA was isolated, first-strand synthesis was used to generate cDNA with an oligo(dT) primer, and endpoint PCR analysis was performed. Primers used for detecting *Dmp1* were the following: forward, 5′-CTGTAGCTGAAAG AGTGGGTA-3′; reverse, 5′-TGTATTATCTTCCAAGCGGGC-3′ (19). PCRs were separated on an agarose gel and stained with ethidium bromide.

RNA and protein stability. Infected MEFs were treated with either 4 μg/ml actinomycin D (Sigma, St. Louis, MO) to assess mRNA stability or 25 μg/ml cycloheximide (Sigma, St. Louis, MO) to assess protein stability. Cells were harvested over a time course of 0, 2, 4, 6, or 8 h posttreatment and subjected, respectively, to RNA isolation, cDNA synthesis reaction, and quantitative reverse transcription-PCR (qRT-PCR) analysis or to Western blot analysis.

Immunoprecipitation. Infected MEFs were freshly harvested, and cells were resuspended and sonicated in EBC lysis buffer (50 mM Tris-HCl, pH 7.4, 120 mM NaCl, 0.5% NP-40, 1 mM EDTA). Then, 300 μg of protein lysate was immunoprecipitated overnight with a rabbit anti-ARF polyclonal antibody or normal rabbit IgG (sc2027; Santa Cruz Biotech-

nology, Santa Cruz, CA). Immune complexes recovered by protein A-Sepharose (GE Healthcare, Piscataway, NJ) were washed three times with EBC buffer and were denatured. Proteins were separated on 12.5% sodium dodecyl sulfate (SDS)-containing polyacrylamide gels and were transferred onto PVDF membranes (Millipore, Boston, MA) and subjected to direct immunoblotting as indicated.

Indirect IF and BrdU incorporation. Infected MEFs were plated onto coverslips. Cells were washed with PBS and fixed at room temperature using 10% formalin–10% methanol, followed by incubation with 1% NP-40 at room temperature for 5 min. Cells were stained with antibodies recognizing ARF (ab26696; Abcam, Cambridge, MA) or MDM2 (op115; Calbiochem/EMD Chemicals, Gibbstown, NJ), followed by the corresponding secondary antibodies conjugated with Alexa Fluor 488 or Alexa Fluor 594 (Invitrogen, Carlsbad, CA), respectively. Cells were then counterstained for nuclei with SlowFade Gold Antifade mounting reagent with 4′,6-diamidino-2-phenylindole (DAPI; Invitrogen, Carlsbad, CA). Fluorescence signals were detected using a Nikon epifluorescent compound microscope fitted with a Nikon FDX-35 charge-coupled-device camera. For measurement of DNA replication, 5-bromodeoxyuridine (BrdU) (Sigma, St. Louis, MO) was added to the culturing medium for 2, 18 or 24 h, as indicated in the figure legends, at a final concentration of 10 μM. Cells were then treated for immunofluorescence (IF) analysis as noted above and additionally incubated with 1.5 N HCl at room temperature for 10 min. A mouse monoclonal antibody recognizing BrdU (Amersham/GE Healthcare, Piscataway, NJ) was used.

Cell proliferation assay, focus formation, and soft-agar formation. For cell proliferation assays, equal numbers of cells (5×10^4 $Dmp1^{-/-}$ MEFs; 1×10^5 $Tsc1^{flox/flox}$ or $Tsc1^{flox/flox}$; $Arf^{-/-}$ MEFs) were replated in triplicate. Every 24 h thereafter, cells were harvested and counted using a hemacytometer. For focus formation, 5×10^3 infected cells were plated in triplicate onto 10-cm² dishes. Cells were grown for 14 days in complete medium and then were fixed with 100% methanol and stained for 30 min with 50% Giemsa. For soft-agar colony formation, 1×10^3 infected cells were seeded in triplicate on 60-mm dishes and allowed to grow for 21 days in complete medium supplemented with fetal bovine serum and Noble agar.

Apoptosis analysis. Infected MEFs were stained with fluorescein isothiocyanate (FITC)-annexin V and propidium iodide using a Dead Cell Apoptosis Kit (V13242; Molecular Probes/Invitrogen, Carlsbad, CA) according to the manufacturer's specifications. Cells were analyzed by flow cytometry using a Becton Dickinson FACSCalibur cell sorter with CELL-Quest Pro (version 5.2) analytical software.

Ribosome fractionation, RNA isolation, and qRT-PCR. Cells were treated with cycloheximide (10 μg/ml) for 5 min before being harvested. Equal numbers of cells (3×10^6) were lysed, and cytosolic extracts were subjected to ribosome fractionation as previously described (33, 46) using a density gradient system (Teledyne ISCO, Lincoln, NE). RNA was isolated from monosome, disome, and polysome fractions using RNAsolv (Omega Bio-Tek, Norcross, GA) according to the manufacturer's specifications. Reverse transcription reactions were performed using a SuperScript III first-strand synthesis system (Invitrogen, Carlsbad, CA) with an oligo(dT) primer. Real-time PCR was performed on an iCycler apparatus (Bio-Rad, Hercules, CA) using SsoFast EvaGreen Supermix (Bio-Rad, Hercules, CA) to amplify *Arf* or *Gapdh* from monosome/disome and polysome fractions. Numbers of *Arf* or *Gapdh* transcripts per fraction were calculated from a standard curve generated from serial dilutions of a known quantity of subcloned *Arf* or *Gapdh* cDNA. *Arf* or *Gapdh* mRNA distribution per fraction was calculated as a percentage of the total number of transcripts in all collected fractions. For the ribosome profiling analysis shown in Fig. 6, cells were treated with puromycin (Sigma, St. Louis, MO) at a final concentration of 1 mM for 3 h.

Tumorigenic assay. Infected MEFs were trypsinized and counted. A total of 2×10^6 cells were resuspended in PBS and injected subcutaneously into the left flank of athymic nude $Foxn1^{nu}/Foxn1^{nu}$ mice. A sample size of five mice per condition was used. Tumor growth was monitored

every day by palpation at the injection site, and the diameter of the tumors was measured in two different planes using a digital caliper. Tumor volume was calculated with the following formula: (height² × length)/2, where height represents the smaller of the two measurements.

Densitometry, image, and statistical analysis. Autofluorograms and immunoblot films were scanned using an ImageScannerIII apparatus (GE Healthcare, Piscataway, NJ), and densities were determined using ImageQuant, version 2005 (GE Healthcare, Piscataway, NJ). Statistical analyses were performed using a Student's *t* test.

RESULTS

ARF is responsive to Ras^V12 and is functional in the absence of *Dmp1*. Previous reports have demonstrated that ARF responds to the Ras^{V12} oncoprotein through a mechanism mediated by the Dmp1 transcription factor (17, 18, 44). However, it was also noted that ARF's induction from Ras^{V12} is compromised, but not completely lost, in the absence of *Dmp1* (16, 18). We sought to further understand the putative regulation and function of ARF in the absence of cooperating transcriptional signals. $Dmp1^{-/-}$ MEFs were infected with a retrovirus encoding Ras^{V12} and harvested at 5 days postinfection for gene expression analysis; confirmation of *Dmp1*-null status of the MEFs was performed by PCR analysis of reverse transcribed cDNA (Fig. 1A). Consistent with prior findings (16, 18), we observed that ARF protein is still increased in response to Ras^{V12} overexpression in the absence of *Dmp1* (Fig. 1B). Strikingly, *Arf* mRNA levels were not significantly altered from Ras^{V12} overexpression in *Dmp1*-deficient cells (Fig. 1C). Collectively, these data indicate that transcriptional activation of *Arf* gene expression is not obligatory for inducing ARF protein levels in response to Ras^{V12}. These observations also indicate that the Ras/Dmp1 pathway is not the only mechanism by which ARF can sense the oncogenic cues of Ras^{V12} signaling.

Since ARF is sensitive to the oncogenic stimulus of Ras^{V12} in *Dmp1*-null cells, we hypothesized that basal ARF could still exert its important antiproliferative functions in these cells. To test this, we infected $Dmp1^{-/-}$ MEFs with a lentivirus encoding a short hairpin targeting a scrambled control or *Arf* exon 1β (siScramble and siARF, respectively) (1), the ARF-specific exon of the *CDKN2A* locus. As shown by Western blot analysis, ARF protein levels were dramatically reduced (~90%) compared to those of the scrambled control (Fig. 2A). To determine the effect of acute knockdown of ARF on cellular proliferation, equal numbers of $Dmp1^{-/-}$ MEFs expressing the short hairpin against *Arf* or scrambled control were seeded in triplicate, and total numbers of cells were counted over 5 days. Acute knockdown of ARF significantly increased the rate of proliferation of $Dmp1^{-/-}$ MEFs (Fig. 2B). Additionally, 5-bromodeoxyuridine (BrdU) incorporation was also monitored to measure the extent of cells entering S phase (Fig. 2C and D). Acute knockdown of ARF caused a significant increase in the percentage of cells undergoing DNA replication; this was observed with both a short (2 h) and a longer (18 h) pulse of BrdU (Fig. 2D and C, respectively). Acute knockdown of ARF did not dramatically alter the amount of cells undergoing apoptosis (4.6% for $Dmp1^{-/-}$ MEFs infected with siScramble-encoding virus and 3% for siARF-encoding virus) (Fig. 2E).

Ras/TSC/mTORC1 pathway can regulate ARF. Our data indicate that ARF is induced in response to oncogenic Ras^{V12} independently of Dmp1 transcriptional activity. We hypothesized that the mTORC1 signal transduction pathway could potentially regulate ARF expression. This critical cell growth regulatory pathway coordinates ribosome biogenesis and mRNA translation. Regula-
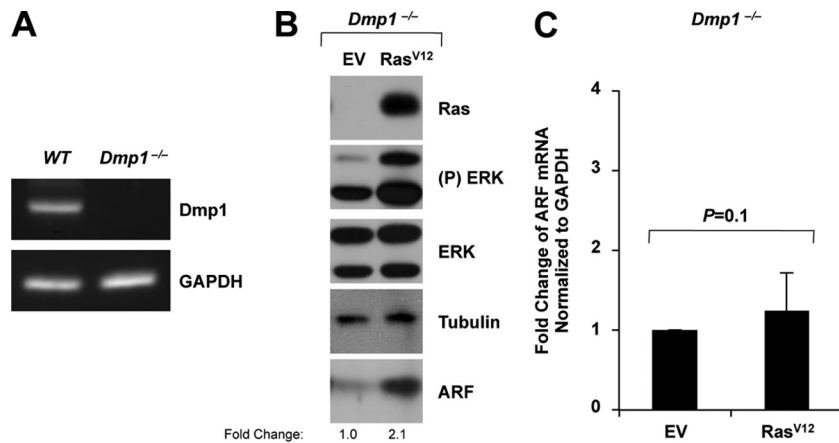
FIG 1 In the absence of *Dmp1*, Ras^{V12} induces ARF protein, but not ARF mRNA. (A) First-strand cDNA was synthesized from total RNA isolated from wild-type (WT) or *Dmp1*$^{-/-}$ MEFs, and endpoint PCR analysis was performed using primers specific for *Dmp1* or *Gapdh*. PCRs were separated on an agarose gel and stained with ethidium bromide. (B and C) *Dmp1*$^{-/-}$ MEFs were transduced with retroviruses encoding an empty vector control (EV) or Ras^{V12} and were harvested at 5 days postinfection for gene expression analysis. (B) Infected cells were lysed, and separated proteins were immunoblotted for the indicated proteins. Expression fold change over empty vector is indicated (B). First-strand cDNA was synthesized from isolated total RNA, and quantitative RT-PCR analysis was performed. *Arf* mRNA levels were normalized to *Gadph* mRNA levels. Fold change was calculated using the $\Delta\Delta C_T$ method. Data are the mean $\pm$ standard deviation of five independent experiments, and *P* values were calculated using the Student *t* test (C). (P), phosphorylated.

tion by this pathway is often associated with translational control of target genes whose protein levels, but not mRNA levels, are modulated in particular cellular contexts (10, 24, 43). To begin evaluating this pathway, wild-type and *Dmp1*$^{-/-}$ MEFs were transduced with a retrovirus encoding Ras^{V12} and subsequently treated with rapamycin, the pharmacological inhibitor of mTORC1 signaling, for 24 h prior to harvesting (Fig. 3A and B). Repressed levels of phospho-S6K1 (Thr 389) and phospho-S6 (Ser 240/244) revealed that mTORC1 signaling was disrupted by rapamycin exposure (Fig. 3A and B). For strains of both genotypes, the induced levels of ARF protein expression were sensitive to rapamycin treatment (Fig. 3A and B), suggesting that mTORC1 signaling is essential for ARF's induction from Ras.

We next wanted to interrogate the involvement of the Ras/mTORC1 pathway in regulating ARF protein levels using genetic manipulations. Tuberous sclerosis complex 1 (TSC1) is an upstream member of the mTORC1 pathway. TSC1 forms a complex with TSC2 that negatively regulates mTORC1 signal transduction (48). We hypothesized that activation of the mTORC1 pathway by acute knockdown of TSC1 would induce ARF protein levels. To test this, wild-type MEFs were infected with lentiviruses encoding small interfering RNAs (siRNAs) recognizing *Tsc1*. Two hairpins were used to reduce TSC1 expression (Fig. 3C). ARF protein levels were upregulated from transient knockdown of TSC1 in a dose-dependent manner (Fig. 3C). Additionally, *Tsc1*$^{flox/flox}$ MEFs were infected with adenoviruses encoding Cre recombinase or a β-galactosidase (LacZ) control. Enhanced levels of phospho-S6K1 (Thr 389) and phospho-S6 (Ser 240/244) demonstrated that hyperactivation of mTORC1 signaling occurred from loss of *Tsc1* (Fig. 3D). Genetic ablation of *Tsc1* also caused an increase in ARF protein levels (Fig. 3D), corroborating the results observed from using RNAi against *Tsc1*. Moreover, we infected wild-type MEFs with Ad-LacZ or Ad-Cre to ensure that this finding was not a nonspecific effect of Cre recombinase or the adenoviral infection protocol (Fig. 3E). Additionally, *Tsc1*$^{+/flox}$ and *Tsc1*$^{flox/flox}$ MEFs were infected with Ad-Cre or Ad-LacZ to evaluate a dose-dependent loss of *Tsc1* on ARF protein levels (Fig. 3F). Loss of one

copy of *Tsc1* was sufficient to induce ARF protein expression, while loss of both copies of *Tsc1* induced ARF protein expression to a greater extent (Fig. 3F).

To investigate whether the ARF induction observed from the loss of *Tsc1* is dependent on TSC/mTORC1 signaling, we infected *Tsc1*$^{flox/flox}$ MEFs with Ad-Cre or the Ad-LacZ control and then treated them with rapamycin for 24 h prior to harvesting. Diminished levels of phospho-S6K1 (Thr 389) and phospho-S6 (Ser 240/244) demonstrated that rapamycin successfully blocked mTORC1 signaling (Fig. 3G). As seen before with infection with a retrovirus encoding Ras^{V12} (Fig. 3A and B), ARF protein levels induced from the loss of *Tsc1* were sensitive to rapamycin treatment (Fig. 3G).

To confirm the contributions of mTORC1 signaling following *Tsc1* deletion to regulation of ARF, RNA interference was used to acutely knockdown *Raptor* or *Rictor* (Fig. 3H and I). Acute knockdown of *Raptor*, but not *Rictor*, abrogated the induction of ARF expression from the ablation of *Tsc1* (Fig. 3H and I). These data provide further support that mTORC1, but not mTORC2, is necessary for mediating the induction of ARF from the loss of *Tsc1*. Taken together, these data demonstrate that hyperactivation of Ras/TSC/mTORC1 pathway can regulate ARF protein levels.

ARF induction from mTORC1 hyperactivation uses a novel translational mechanism. Given that mTORC1 signal transduction plays a crucial role in the translational regulation of specific mRNA transcripts, we hypothesized that this might be an underlying mechanism responsible for inducing ARF protein levels. To test this, we assessed different aspects of *Arf* gene expression in the face of mTORC1 hyperactivation. For each of these experiments, *Tsc1*$^{flox/flox}$ MEFs were infected with Ad-Cre or Ad-LacZ as before. Despite the increases in ARF protein expression, no significant changes were observed in *Arf* mRNA levels following *Tsc1* loss (Fig. 4A). Next, we evaluated *Arf* mRNA stability and observed a rate of *Arf* mRNA decay that was nearly identical in Ad-LacZ- and Ad-Cre-infected *Tsc1*$^{flox/flox}$ cells (Fig. 4B). Moreover, the rate of ARF protein decay was faster in Ad-Cre-infected *Tsc1*$^{flox/flox}$ MEFs than in Ad-LacZ-infected cells (Fig. 4C and D), suggesting that a higher rate of ARF protein must be synthesized in order to in-
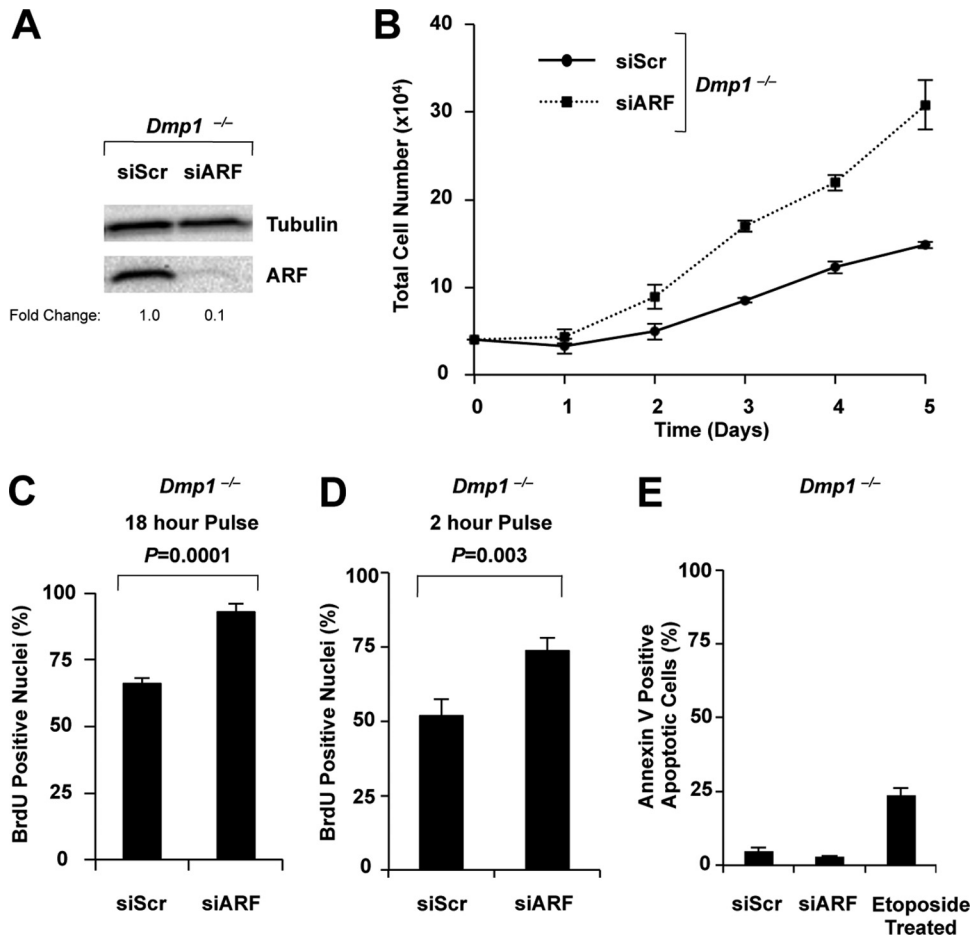
FIG 2 ARF remains functional in the absence of *Dmp1*. *Dmp1*$^{-/-}$ MEFs were infected with lentiviruses encoding a short hairpin against *Arf* (siARF) or the siScramble control (siScr). (A) Infected cells were lysed, and separated proteins were immunoblotted for the indicated proteins. Expression fold change over the siScramble control is indicated. (B) A total of 5×10^4 cells were seeded in triplicate for each indicated time point. Cells were trypsinized and counted with a hemacytometer each day for 5 days thereafter. (C and D) Infected cells were seeded on coverslips and were pulsed with BrdU for 18 or 2 h, as indicated. Indirect immunofluorescence analysis was used to score BrdU incorporation. Representative data are depicted as the mean ± standard deviation of 50 nuclei counted in triplicate, and *P* values were calculated using the Student *t* test. (E) Infected cells were harvested and stained with FITC-annexin V and propidium iodide and subjected to flow cytometry analysis. Representative data are expressed as the mean ± standard deviation of 10,000 events performed in triplicate, and *P* values were calculated using the Student *t* test.

crease steady-state levels in the cell. We also assessed the rate of protein decay of ectopic HA-ARF expressed in Ad-Cre-infected *Tsc1*$^{flox/flox}$; *Arf*$^{-/-}$ MEFs (Fig. 4E and F) and noted a similarly accelerated half-life for HA-ARF (~4 h). This observation supports the notion that ARF protein is being degraded at a high rate in the absence of *Tsc1* compared to ARF's normally observed half-life of ~6 h (25).

To further test the hypothesis that translational regulation could be the molecular mechanism responsible for eliciting ARF's induction from mTORC1 hyperactivation, we assessed the association of *Arf* mRNA with actively translating polyribosomes. To accomplish this task, cytosolic ribosomes were isolated by sucrose gradient centrifugation from equal numbers of *Dmp1*$^{-/-}$ MEFs infected with a retrovirus encoding either Ras^{V12} or an empty vector control (Fig. 5A and B). Ribosomal subunits were detected by measuring RNA absorbance at 254 nm by continuous UV monitoring (Fig. 5B). To assess the distribution of *Arf* mRNA transcripts in individual fractions comprising isolated monosomes, disomes, or polysomes, total RNA was isolated from each

sucrose gradient fraction, and *Arf* mRNA levels were determined with qRT-PCR. Strikingly, *Arf* mRNA transcripts associated with different polyribosome fractions in *Dmp1*-null cells infected with retroviruses encoding Ras^{V12} and empty vector (Fig. 5C). In *Dmp1*$^{-/-}$ MEFs infected with a Ras^{V12}-encoding retrovirus, *Arf* mRNA was pooled to a heavier polyribosome fraction, indicating that there is a greater extent of *Arf* mRNAs being actively translated by multiple ribosomes (more ribosomes associated per mRNA) in these cells (Fig. 5C). These data support the hypothesis that ARF is translationally regulated in the presence of oncogenic Ras^{V12} signals.

To address the possibility that general gains in global protein translation could account for the increased translation of *Arf* mRNA transcripts, we evaluated the distribution of *Gapdh* mRNA in sucrose gradient fractions in *Dmp1*$^{-/-}$ MEFs infected with a retrovirus encoding either Ras^{V12} or an empty vector control (Fig. 5D). No dramatic differences in the distribution of *Gapdh* mRNA transcripts were observed across isolated monosomes or polyribosomes, in contrast to the distribution observed for *Arf* mRNA (Fig.
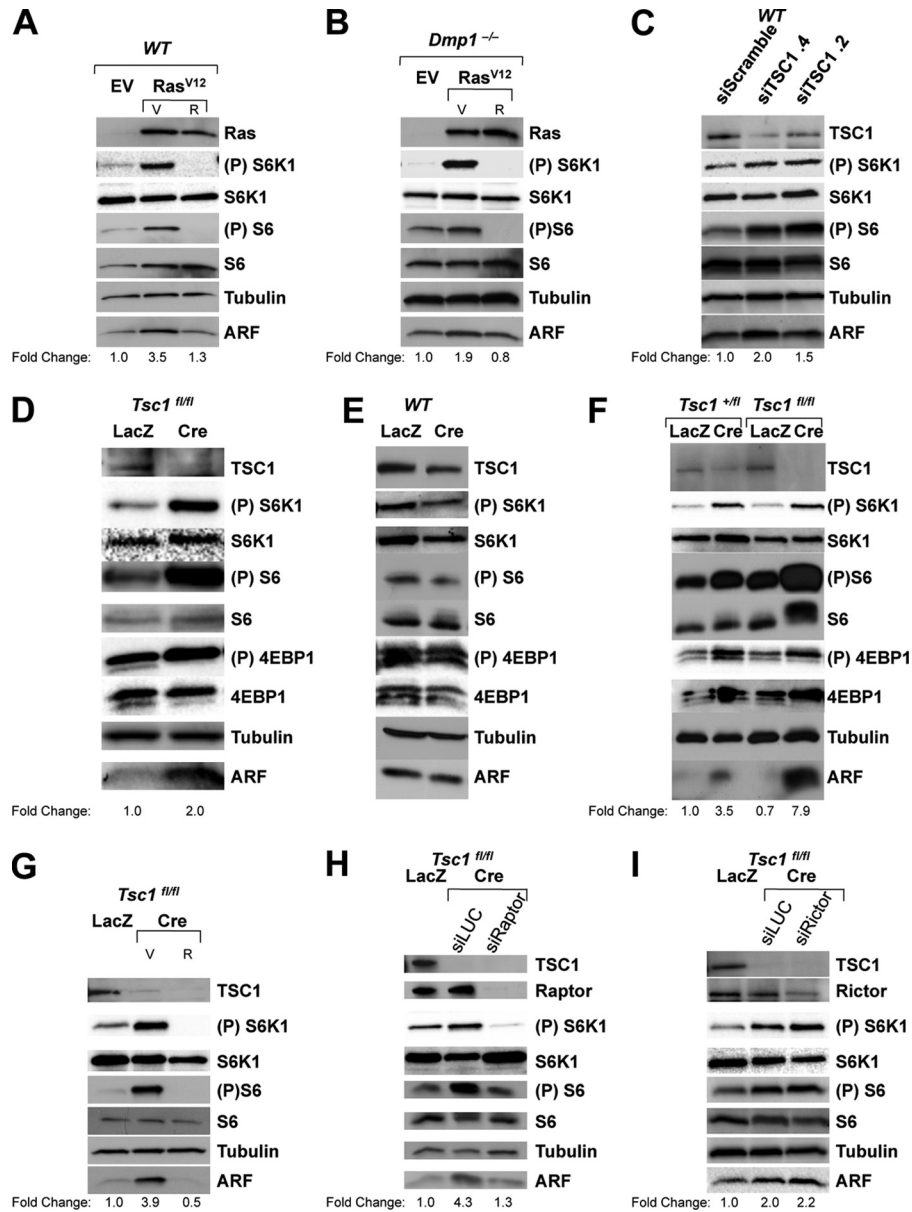
FIG 3 Ras/TSC/mTORC1 pathway can regulate ARF. Infected cells were lysed, and separated proteins were immunoblotted for the indicated proteins. Expression fold change over empty vector (EV), siScramble, or LacZ control is indicated. (A and B) WT or *Dmp1*−/− MEFs were infected with retroviruses encoding an empty vector control or Ras^{V12} and were harvested at 5 days postinfection. Ras^{V12}-infected cells were treated with 100 nM rapamycin (R) or vehicle (V) for 24 h prior to harvesting. (C) Wild-type MEFs were infected with lentiviruses encoding short hairpins against *Tsc1* or the siScramble control and were harvested at 7 days postinfection. (D to F) *Tsc1*$^{flox/flox}$, WT, or *Tsc1*$^{+/flox}$ MEFs (as indicated) were infected with adenoviruses encoding β-galactosidase (LacZ) or Cre recombinase and were harvested at 9 days postinfection. (G to I) *Tsc1*$^{flox/flox}$ MEFs were infected with adenoviruses encoding β-galactosidase (LacZ) or Cre recombinase and harvested at 9 days postinfection. (G) Ad-Cre-infected cells were treated with 100 nM rapamycin (R) or vehicle (V) control for 24 h prior to harvesting. (H and I) Ad-Cre-infected cells were then transduced with viruses encoding short hairpins recognizing *Raptor* (siRaptor) or *Rictor* (siRictor) or a luciferase control (siLUC) at 5 days postinfection and then harvested at 9 days postinfection for Western blot analysis. P, phosphorylated.

5C). This suggests that the gain in *Arf* mRNA association with actively translating polyribosomes is a selective phenotype caused by Ras^{V12} oncogenic signaling in the absence of *Dmp1*.

To confirm that *Arf* mRNA transcripts are actually associating with actively translating polyribosomes, we assessed whether puromycin could release *Arf* mRNA transcripts from the polyribosome fractions. Puromycin treatment causes a block in translation elongation and a premature release of the nascent polypeptide chain from actively translating polyribosomes (2, 45). To accomplish this, *Dmp1*−/− MEFs were infected with blasticidin-resistant retroviral constructs encoding either GFP or Ras^{V12}. Consistent with earlier findings, ARF protein is increased in response to Ras^{V12} overexpression in the absence of *Dmp1* (Fig. 6A). *Dmp1*−/− MEFs infected with a retrovirus encoding GFP or Ras^{V12} were treated with 1 mM puromycin for 3 h (45, 49). Cytosolic ribosomes were isolated by sucrose gradient centrifugation from equal numbers of cells, and ribosomal subunits were monitored as before (Fig. 6B). *Dmp1*−/− MEFs treated with puromycin
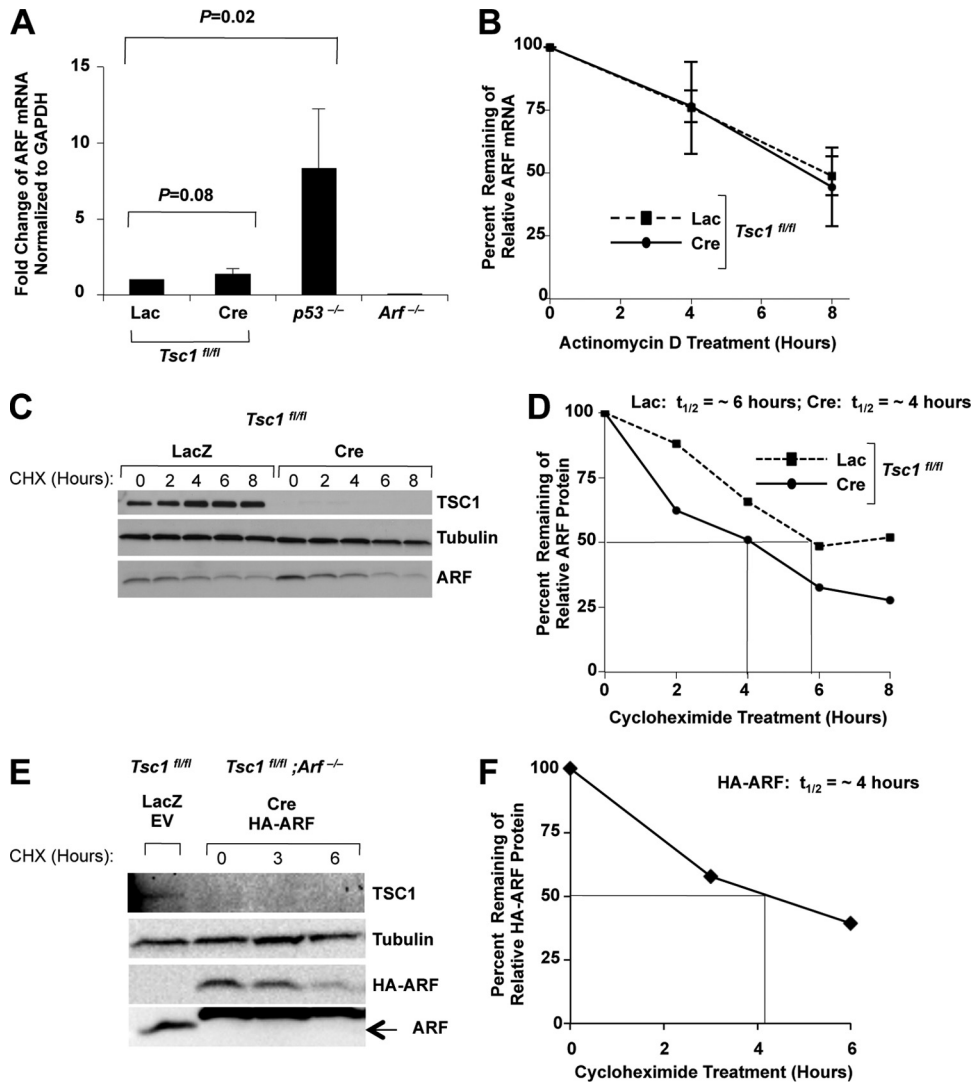
FIG 4 Loss of *Tsc1* does not induce ARF through transcription, mRNA stability, or protein stability. (A to D) *Tsc1^flox/flox* MEFs were infected with adenoviruses encoding β-galactosidase (LacZ) or Cre recombinase and were harvested at 9 days postinfection for gene expression analysis. First-strand cDNA was synthesized from isolated total RNA, and quantitative RT-PCR analysis was performed. *Arf* mRNA levels were normalized to *Gadph* mRNA levels (A). Fold change was calculated using the $\Delta\Delta C_T$ method. Data are the mean ± standard deviation of three independent experiments, and *P* values were calculated using the Student *t* test. (B) Cells were treated with 4 μg/ml actinomycin D for the indicated time points. First-strand cDNA was synthesized from isolated total RNA, and quantitative RT-PCR analysis was performed as described for panel A. Data are represented as percent remaining of *Arf* mRNA normalized to *Gadph* levels relative to the respective zero hour treatment. (C) Cells were treated with 25 μg/ml cycloheximide (CHX) and were harvested at the indicated time points for Western blot analysis. Representative immunoblots are depicted. Densitometry quantification of immunoblots from panel C is depicted in panel D. Data are represented as percent remaining of ARF protein levels normalized to tubulin protein levels relative to the respective 0-h treatment. (E and F) *Tsc1^flox/flox* or *Tsc1^flox/flox*; *Arf^−/−* MEFs were infected with adenoviruses encoding β-galactosidase (LacZ) or Cre recombinase and retroviruses encoding an empty vector control or HA-ARF, as indicated. Cells were treated with 25 μg/ml cycloheximide and were harvested at the indicated time points for Western blot analysis. Representative immunoblots are depicted. In panel F, densitometry quantification of the immunoblots shown in panel E is depicted for cells infected with a retrovirus encoding HA-ARF. Data are represented as percent remaining of HA-ARF protein normalized to tubulin protein levels relative to the 0-h treatment. $t_{1/2}$, half-life.

and infected with GFP- and Ras^V12-encoding retroviruses showed dramatic increases in the amplitude of the 80S peak, along with the complete disappearance of the polysome peaks (Fig. 6B). *Arf* mRNA distribution in fractions was then determined (Fig. 6C and D). *Arf* mRNA distribution in puromycin-treated, GFP-expressing cells mimicked the distribution of *Arf* mRNA in untreated GFP-expressing cells (Fig. 6C). This surprising finding suggests that *Arf* mRNA found on the polysome peaks in these GFP-expressing cells could in fact be "pseudo-polysomes" as opposed to actual polyribosomes (49). In contrast, puromycin treatment released *Arf* mRNA from the polysome peaks in *Dmp1^−/−* MEFs infected with Ras^V12-encoding retrovirus (Fig. 6D), indicating that *Arf* mRNA transcripts are indeed associating with actively translating polyribosomes in response to oncogenic Ras^V12 signaling.

To determine whether inhibition of mTORC1 signaling could similarly displace *Arf* mRNA distribution from polysome peaks, *Dmp1^−/−* MEFs were transduced with a retrovirus encoding
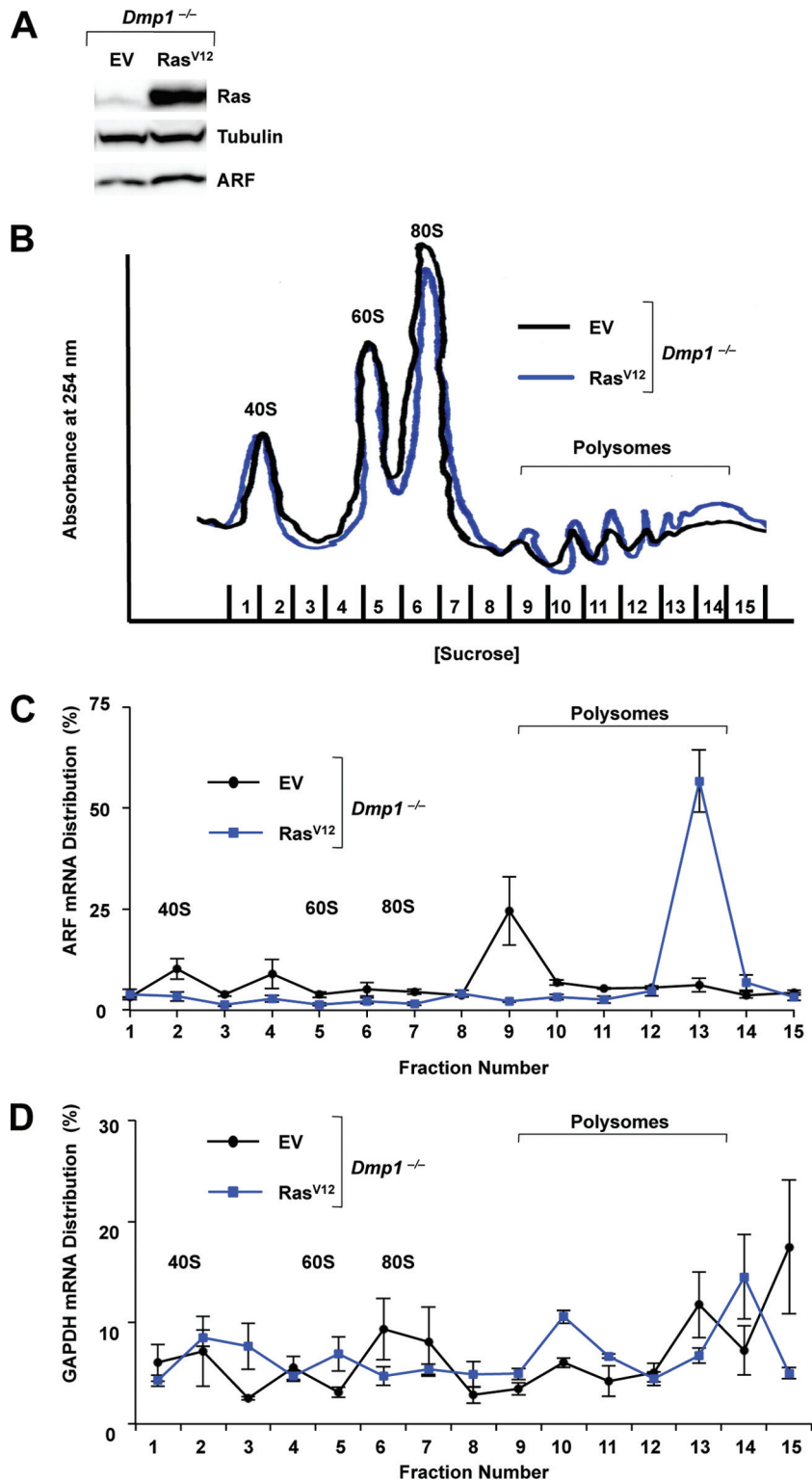
FIG 5 *Arf* mRNA association with actively translating polyribosomes increases from Ras[V12] signaling in the absence of *Dmp1*. *Dmp1*^{−/−} MEFs were transduced with retroviruses encoding an empty vector control (EV) or Ras[V12] and were harvested at 5 days postinfection. Cytosolic extracts from equal number of cells (3 × 10^6) treated for 5 min with cycloheximide (10 μg/ml) were separated on 7 to 47% sucrose gradients with constant UV monitoring (254 nm). (A) Excess cells were lysed, and separated proteins were immunoblotted for the indicated proteins. (B) A representative graph depicts the A_{254} absorbance of ribosome subunits over increasing sucrose density. (C) Total RNA was isolated from each sucrose gradient fraction, and first-strand cDNA was synthesized for each fraction. Monosome-, disome-, and polysome-associated *Arf* mRNA levels were measured with qRT-PCR and were calculated as a percentage of total *Arf* mRNA collected in all fractions. Data are the mean ± standard error of the mean of three independent experiments. (D) Monosome-, disome-, and polysome-associated *Gapdh* mRNA levels were measured as described for panel C.
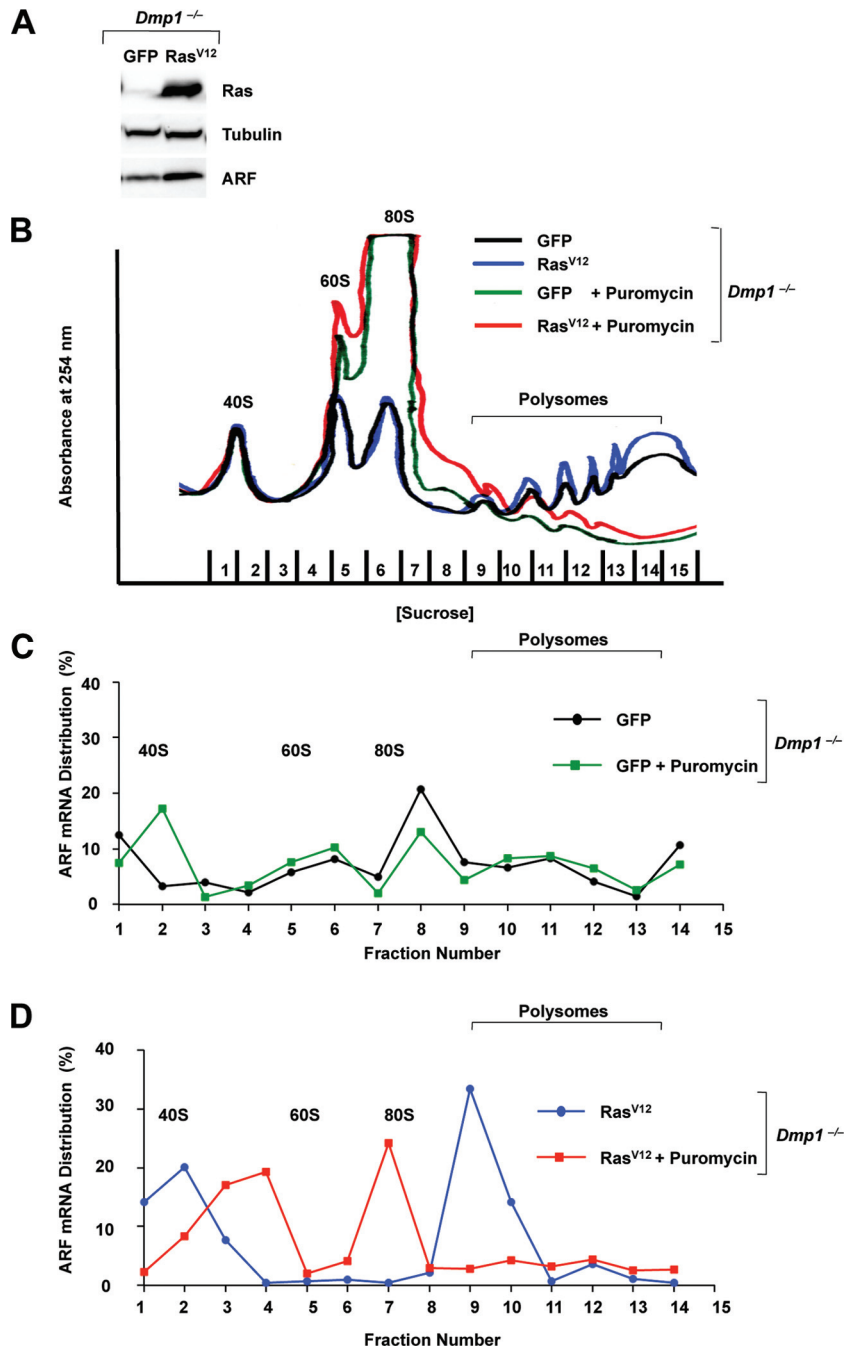
FIG 6 *Arf* mRNA association with actively translating polyribosomes caused by hypergrowth stimuli can be disrupted with puromycin exposure. Retroviruses were generated with pWZL-GFP-IRES-blast or pWZL-Ras^{V12}-IRES-blast. $Dmp1^{-/-}$ MEFs were transduced with these retroviruses, and infected cells were analyzed at 5 days postinfection. Cells were treated with 1 mM puromycin for 3 h, and then cytosolic extracts from equal numbers of cells (3×10^6) treated for 5 min with cycloheximide (10 μg/ml) were separated on 7 to 47% sucrose gradients with constant UV monitoring (254 nm). (A) Excess untreated cells were lysed, and separated proteins were immunoblotted for the indicated proteins. (B) A representative graph depicts the A_{254} absorbance of ribosome subunits over increasing sucrose density. (C) Total RNA was isolated from each sucrose gradient fraction, and first-strand cDNA was synthesized for each fraction. Monosome-, disome-, and polysome-associated *Arf* mRNA levels were measured with qRT-PCR and were calculated as a percentage of total *Arf* mRNA collected in all fractions. (D) Monosome-, disome-, and polysome-associated *Arf* mRNA levels were measured as described for panel C.

Ras^{V12} and subsequently treated with rapamycin for 24 h prior to harvesting. Ribosomal subunits were monitored as before (Fig. 7A and B). Although rapamycin did not completely displace *Arf* mRNA from translating polyribosomes, rapamycin treatment did shift *Arf* mRNA away from the heavy polyribosome fractions,

where it accumulates in response to Ras^{V12} (Fig. 7C). This finding demonstrates the sensitivity of *Arf* mRNA association with translating polyribosomes to rapamycin exposure. To further interrogate the effects of mTORC1 signaling on the association of *Arf* mRNA with actively translating polyribosomes, *Tsc1$^{flox/flox}$* MEFs
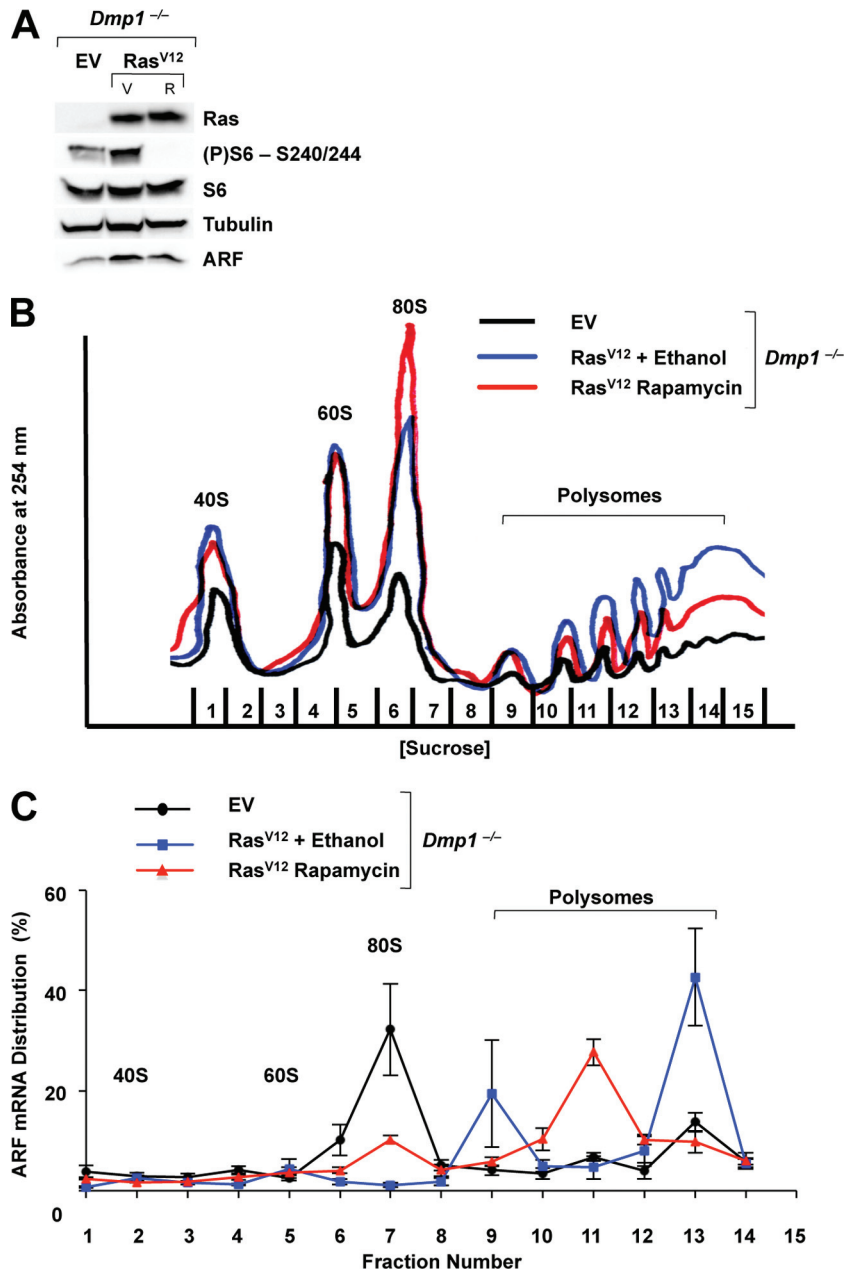
FIG 7 *Arf* mRNA is partially displaced from actively translating polyribosomes by rapamycin exposure. *Dmp1*⁻/⁻ MEFs were transduced with retroviruses encoding an empty vector control (EV) or Ras^V12 and were harvested at 5 days postinfection. Cells infected with Ras^V12-encoding virus were treated with 100 nM rapamycin (R) or vehicle (V) for 24 h prior to harvesting. Cytosolic extracts from equal numbers of cells (3×10^6) treated for 5 min with cycloheximide (10 μg/ml) were separated on 7 to 47% sucrose gradients with constant UV monitoring (254 nm). (A) Excess cells were lysed, and separated proteins were immunoblotted for the indicated proteins. (B) A representative graph depicts the A_{254} absorbance of ribosome subunits over increasing sucrose density. (C) Total RNA was isolated from each sucrose gradient fraction, and first-strand cDNA was synthesized for each fraction. Monosome-, disome-, and polysome-associated *Arf* mRNA levels were measured with qRT-PCR and were calculated as a percentage of total *Arf* mRNA collected in all fractions. Data are the mean ± standard error of the mean of three independent experiments. (P), phosphorylated.

were infected with Ad-Cre or the Ad-LacZ control and were subjected to ribosome profiling (Fig. 8A and B). We found that more *Arf* mRNA pooled to heavier polyribosome fractions upon the loss of *Tsc1* (Fig. 8C). Taken together, these findings support the hypothesis that ARF is translationally regulated in the presence of hyperactivated Ras/TSC/mTORC1 signaling.

ARF induction activates a p53 response. To determine

whether the ARF protein translationally induced from *Tsc1* loss is functional, we assessed several aspects of ARF biology. ARF binds to and sequesters MDM2 in the nucleolus, allowing p53 protein levels to accumulate and become active in the nucleoplasm (53). *Tsc1*^flox/flox MEFs infected with Ad-Cre or the Ad-LacZ control were analyzed for MDM2 and ARF colocalization (Fig. 9A and B). In both Ad-Cre- and Ad-LacZ-infected cells, ARF exhibited nu-
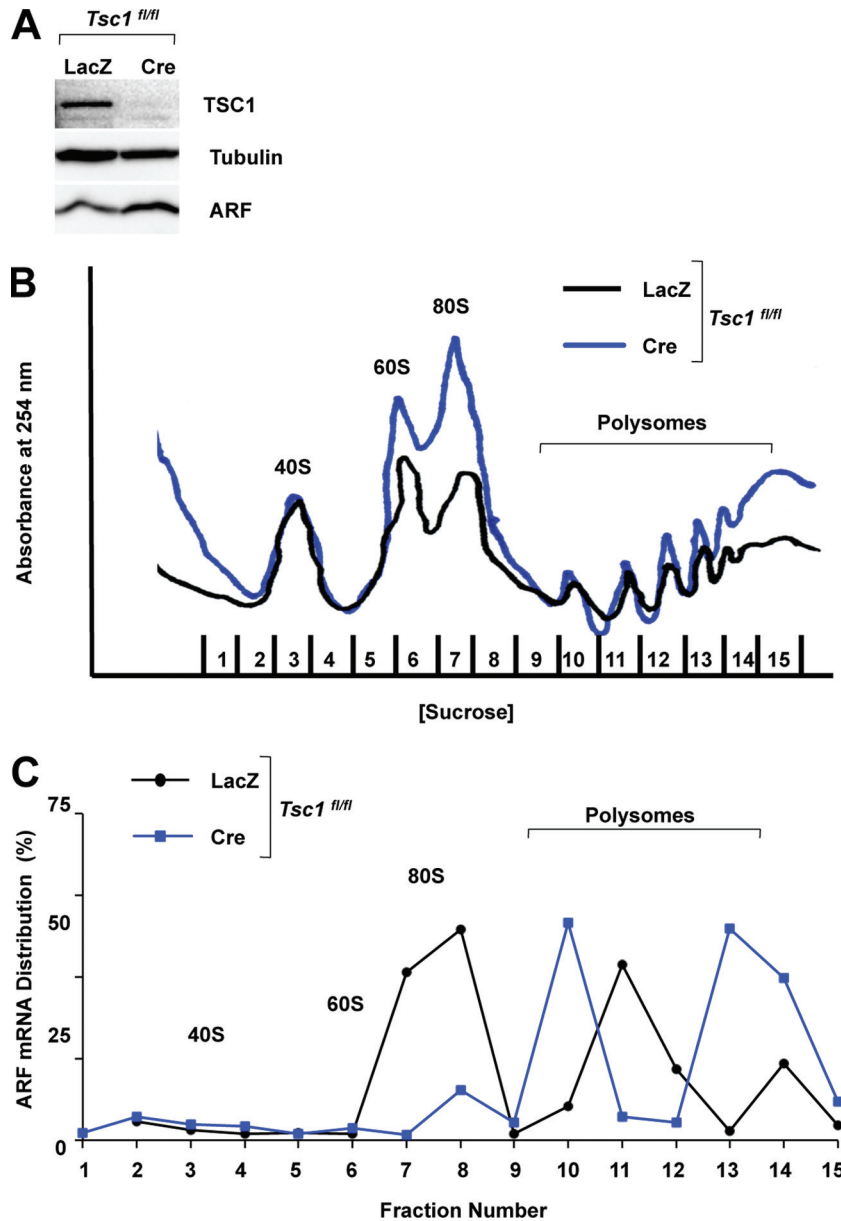
FIG 8 *Arf* mRNA association with actively translating polyribosomes increases from the loss of *Tsc1*. *Tsc1flox/flox* MEFs were infected with adenoviruses encoding β-galactosidase (LacZ) or Cre recombinase and harvested at 9 days postinfection. Cytosolic extracts from equal numbers of cells (3×10^6) treated for 5 min with cycloheximide (10 μg/ml) were separated on 7 to 47% sucrose gradients with constant UV monitoring (254 nm). (A) Excess cells were lysed, and separated proteins were immunoblotted for the indicated proteins. (B) A representative graph depicts the A_{254} of ribosome subunits over increasing sucrose density. (C) Total RNA was isolated from each sucrose gradient fraction, and first-strand cDNA was synthesized for each fraction. Monosome-, disome-, and polysome-associated *Arf* mRNA levels were measured with qRT-PCR and were calculated as a percentage of total *Arf* mRNA collected in all fractions.

cleolar subcellular localization (Fig. 9A and B). Furthermore, we found that ARF and MDM2 had increased colocalization in nucleoli in Ad-Cre-infected *Tsc1flox/flox* MEFs compared to levels in Ad-LacZ-infected cells (Fig. 9A and B). Next, ARF-MDM2 complexes were immunoprecipitated from infected *Tsc1flox/flox* lysates with a polyclonal antibody recognizing ARF and immunoblotted for MDM2 (Fig. 9C). Induced ARF protein displayed strong binding to MDM2 in Ad-Cre-infected *Tsc1flox/flox* MEFs (Fig. 9C). Collectively, these data suggest that the loss of *Tsc1* increases ARF protein expression and its ability to bind to and relocalize MDM2 into the nucleolus.

To examine whether this increase in ARF-MDM2 binding resulted in p53 activation, infected *Tsc1flox/flox* lysates were probed for p53 and two of its downstream target genes, p21 and MDM2. p53, MDM2, and p21 displayed 2-fold increases in protein levels following *Tsc1* loss (Fig. 9D). Similarly, the induction of p53, p21, and MDM2 was completely abrogated in Ad-Cre-infected *Tsc1flox/flox*; *Arf−/−* MEFs (Fig. 9D), implying that ARF is necessary for facilitating the induction of p53 and its target genes in response to *Tsc1* loss. Alternatively, infected *Tsc1flox/flox* MEFs were treated with rapamycin 24 h prior to harvesting. The induction of ARF caused by the loss of *Tsc1* was disrupted due to rapamycin expo-
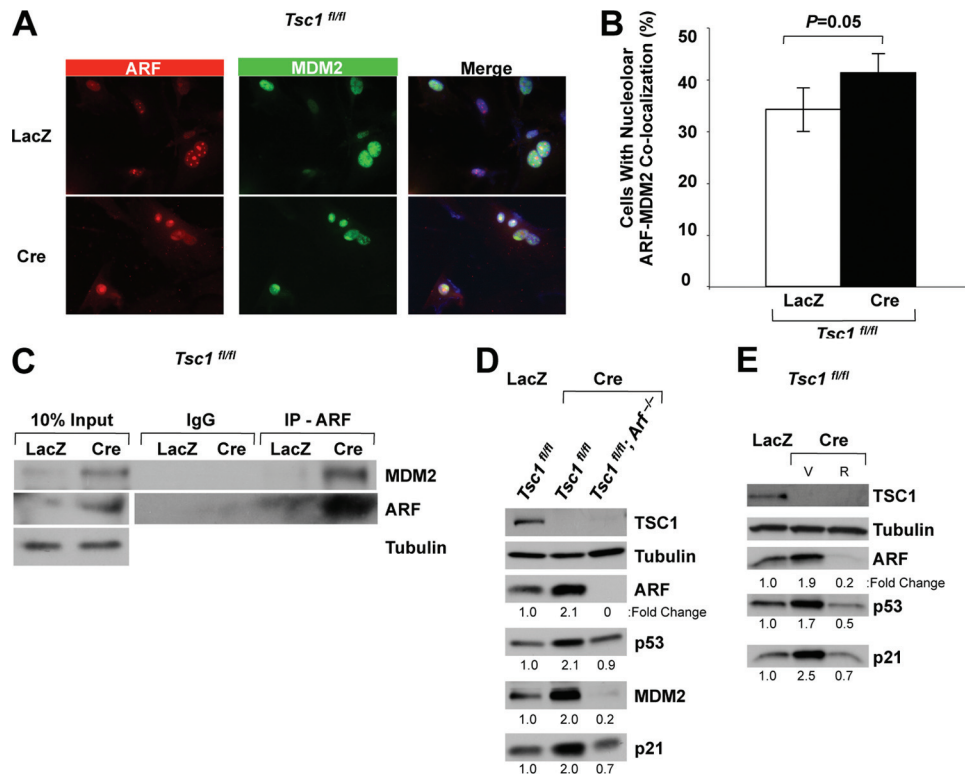
FIG 9 ARF induced from hypergrowth stimuli activates a p53 response. *Tsc1^{flox/flox}* MEFs were infected with adenoviruses encoding β-galactosidase (LacZ) or Cre recombinase and were harvested at 9 days postinfection for analysis. (A) Infected cells were seeded onto coverslips, fixed, and stained for indirect immunofluorescence analysis with specific primary antibodies for ARF and MDM2 and for Alexa Fluor 594 and Alexa Fluor 488, respectively. Cells were counterstained for nuclei with SlowFade Gold Antifade mounting reagent with DAPI. (B) Quantification of nucleolar ARF-MDM2 colocalization is depicted from indirect immunofluorescence analysis as described for panel A. Representative data are expressed as the mean ± standard deviation of 50 nuclei counted in triplicate, and *P* values were calculated using the Student *t* test. (C) Lysates from infected cells were immunoprecipitated with a rabbit polyclonal antibody directed against ARF or normal rabbit IgG. Proteins immune complexes were separated, transferred to PVDF membranes, and immunoblotted with the indicated antibodies. (D and E) Infected cells were lysed, and separated proteins were immunoblotted for indicated proteins. Expression fold change over the LacZ control is indicated (D). Ad-Cre-infected cells were treated with 100 nM rapamycin (R) or vehicle (V) control for 24 h prior to harvesting (E).

sure (Fig. 9E), and, consequently, the induction of p53, p21, and MDM2 was similarly abrogated in the absence of ARF induction (Fig. 9E).

ARF/p53 response causes cell cycle arrest. Given that hyperactivation of mTORC1 signaling increases ARF protein expression and that ARF induces p53 and its downstream targets, we hypothesized that ARF was responsible for eliciting a cell cycle arrest in response to mTORC1 hyperactivation. To test this, cell proliferation was monitored each day for 6 days. The rate of proliferation of Ad-Cre-infected *Tsc1^{flox/flox}* MEFs was markedly reduced compared to that of Ad-LacZ-infected cells (Fig. 10A and B), consistent with the ARF-dependent activation of p53 (Fig. 9). However, this proliferation defect was absent upon *Tsc1* loss in cells also lacking *Arf* (Fig. 10B). Of note, changes in cell death (Fig. 10C) do not account for the decrease in total cell number observed in Ad-Cre-infected *Tsc1^{flox/flox}* cells. Additionally, BrdU incorporation was measured (Fig. 10D). As seen before, Ad-Cre-infected *Tsc1^{flox/flox}* MEFs exhibited a significant decrease in BrdU incorporation compared to Ad-LacZ-infected cells (Fig. 10D). Notably, this decrease was completely rescued in the absence of *Arf* (Fig. 10D). Furthermore, acute knockdown of TSC1 reduced BrdU incorporation in wild-type MEFs (Fig. 10E), corresponding with their dose-dependent induction of ARF protein (Fig. 3C).

Since ARF serves to prevent proliferation in response to loss of *Tsc1*, we hypothesized that removal of ARF would permit cells with hyperactivated mTOR to proliferate long-term without being properly checked. To test this, *Tsc1^{flox/flox}*; *Arf^{-/-}* MEFs were infected with Ad-Cre or the Ad-LacZ control and subjected to long-term focus formation analysis (Fig. 10F and G). Significantly more foci formed by hyperactivating mTOR signaling in *Arf^{-/-}* cells, and there was an increase in total focus area (Fig. 10H and I). Taken together, this indicates that ARF keeps cell proliferation in check by responding to heightened levels of mTORC1 signaling to induce cell cycle arrest.

Translationally regulated ARF represses transformation and tumorigenesis. The observation that ARF induces a p53-mediated cell cycle arrest in response to hypergrowth cues emanating from hyperactivation of mTORC1 signal transduction led us to test the hypothesis that ARF could inhibit transformation and tumorigenesis in response to these hypergrowth cues. We infected *Dmp1^{-/-}* MEFs or *Arf^{-/-}* MEFs with a retrovirus encoding Ras^{V12} or an empty vector control and assessed anchorage-independent growth in soft agar (Fig. 11A). In MEFs infected with Ras^{V12}-encoding virus, *Dmp1^{-/-}* cells formed significantly fewer colonies in soft agar than *Arf^{-/-}* cells (Fig. 11B). To determine if the induced levels of ARF in *Dmp1^{-/-}* MEFs infected with Ras^{V12}-encoding virus were responsible for the inhibition of colony formation, infected *Dmp1^{-/-}* MEFs were also transduced with virus encoding an siRNA recognizing ARF or a scrambled
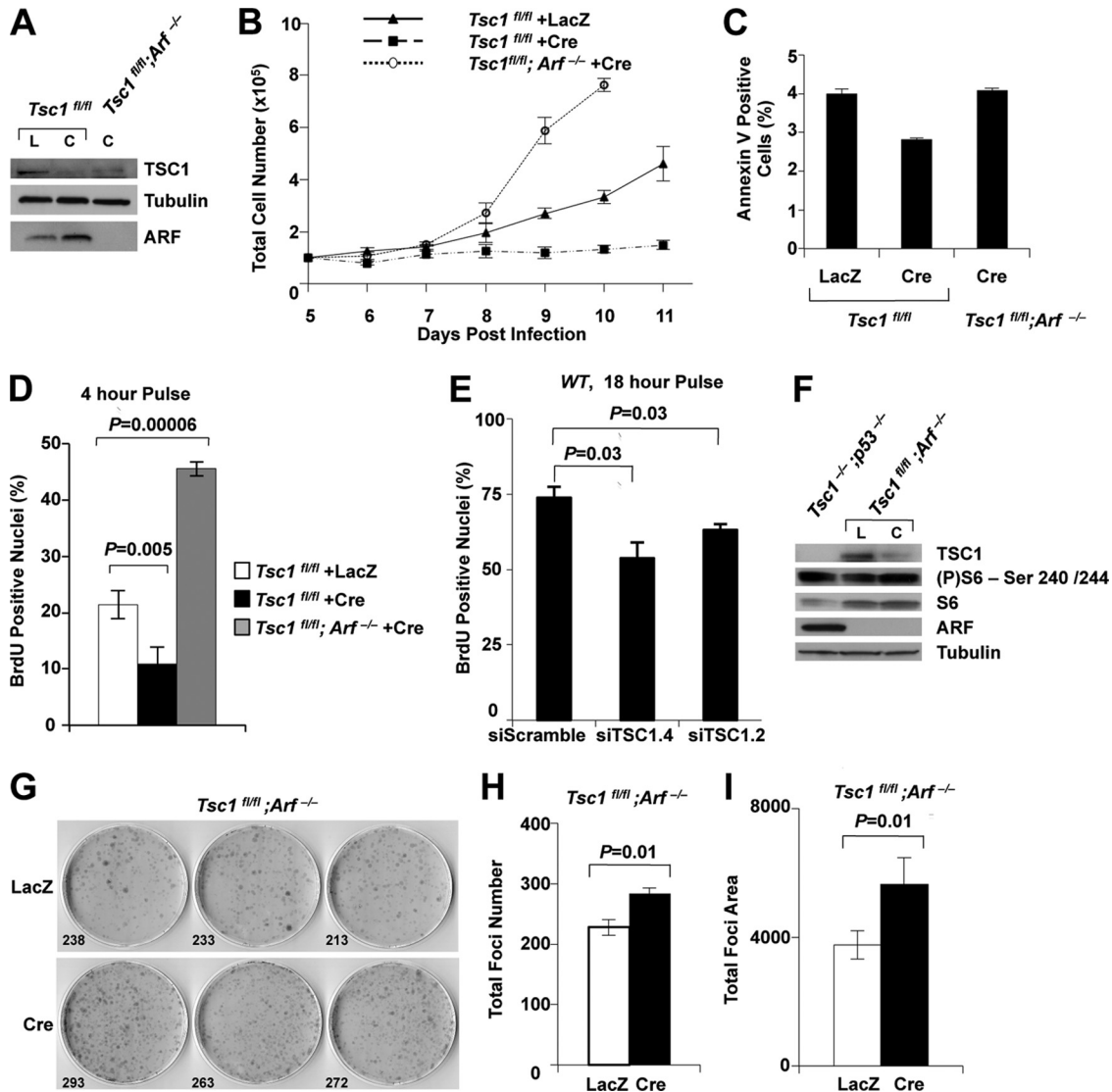
FIG 10 ARF/p53 response induces a cell cycle arrest. (A to D) *Tsc1^flox/flox* or *Tsc1^flox/flox*; *Arf^−/−* MEFs were infected with adenoviruses encoding β-galactosidase (LacZ) or Cre recombinase as indicated. Infected cells were lysed, and separated proteins were immunoblotted for indicated proteins (A). A total of 1×10^5 cells were seeded in triplicate for each indicated time point at 5 days postinfection. Cells were then trypsinized and counted with a hemacytometer each day for 6 days thereafter (B). Infected cells were harvested and stained with FITC-annexin V and propidium iodide and subjected to flow cytometry analysis (C). Representative data are depicted as the mean ± standard deviation of 10,000 events performed in triplicate. (D) Infected cells were seeded on coverslips at 9 days postinfection. On day 10 postinfection, cells were pulsed with BrdU for 4 h. Indirect immunofluorescence analysis was used to score BrdU incorporation. Representative data are expressed as the mean ± standard deviation of 50 nuclei counted in triplicate, and *P* values were calculated using the Student *t* test. (E) Wild-type MEFs were infected with lentiviruses encoding short hairpins against *Tsc1* or the siScramble control and were seeded on coverslips at 7 days postinfection for BrdU incorporation. Cells were pulsed with BrdU for 18 h, and analysis was performed as described for panel D. (F to I) *Tsc1^flox/flox*; *Arf^−/−* MEFs were infected with adenoviruses encoding β-galactosidase (LacZ [L]) or Cre recombinase (C) as indicated. A total of 5×10^3 cells were seeded in triplicate onto 10-cm² dishes for focus formation analysis. Infected cells were lysed, and separated proteins were immunoblotted for the indicated proteins (F). Cells were grown for 14 days in complete medium and were fixed and stained with Giemsa (G). Panels H and I show, respectively, the quantification of the total number of foci and total focus area of representative images from panel G. (P), phosphorylatd.

control. Knockdown of ARF restored the ability of *Dmp1^−/−* MEFs infected with Ras^V12^-encoding virus to form colonies in soft agar, thereby phenocopying the colony-forming potential of infected *Arf^−/−* MEFs (Fig. 11B). No dramatic changes in apoptotic cell death were observed, suggesting that changes in cell death do not account for the differences observed in colony formation (Fig. 11C).

To determine whether translationally regulated ARF could repress tumorigenesis in an allograft model, we assessed tumor formation and burden of *Dmp1^−/−* or *Arf^−/−* MEFs infected

with Ras^V12^-encoding virus by subcutaneously injecting MEFs into the flanks of nude mice (Fig. 11D and E); as before, *Dmp1^−/−* MEFs were also infected with a virus encoding an siRNA recognizing ARF or a scrambled control (siScramble) in order to determine the specificity of ARF's involvement in preventing tumorigenesis (Fig. 11E, inset). Strikingly, tumor onset and growth were markedly reduced in mice injected with *Dmp1^−/−* MEFs infected with siScramble-encoding virus compared to *Arf^−/−* MEFs (Fig. 11D and E). Furthermore, acute
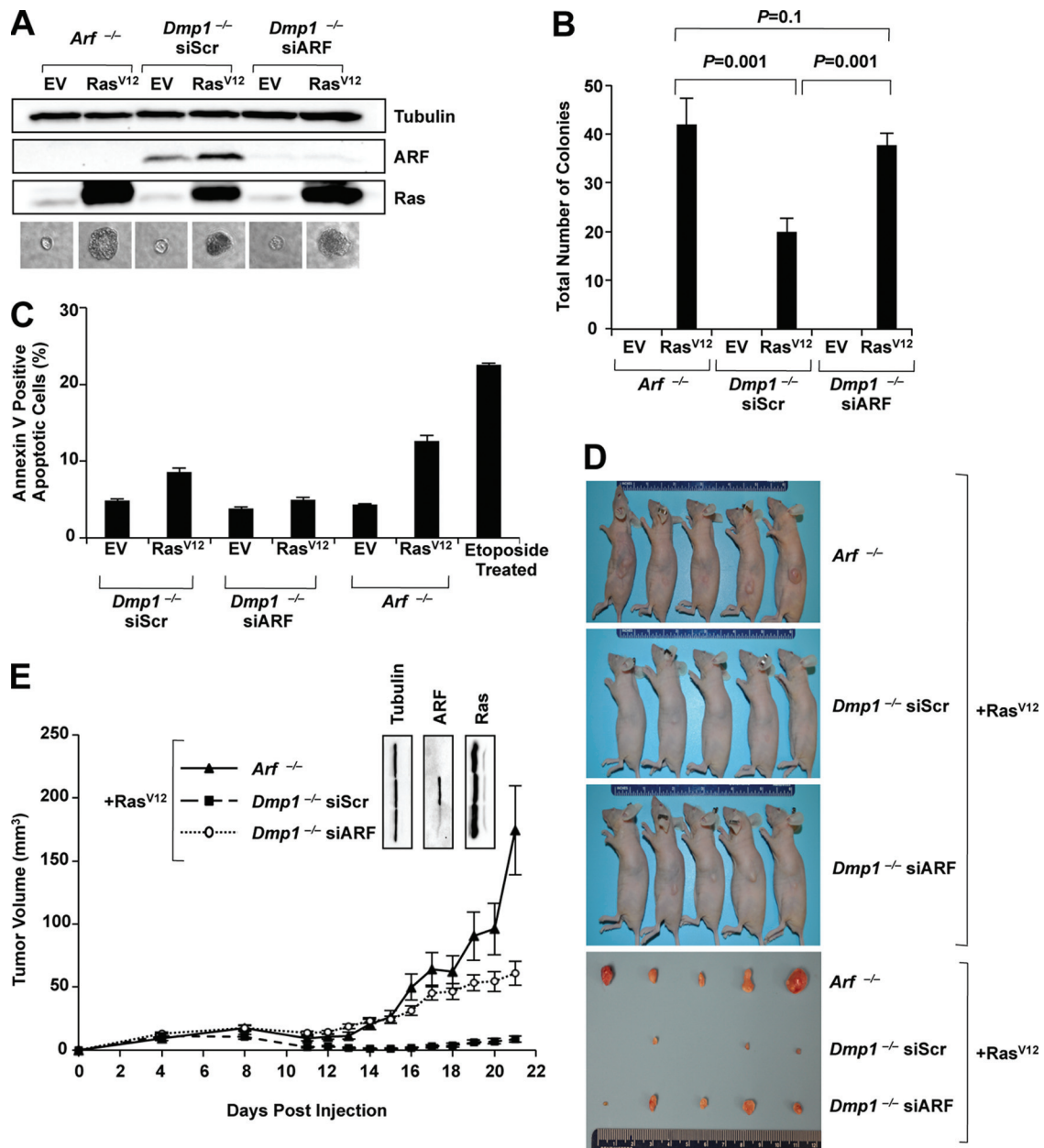
FIG 11 ARF induced from hypergrowth cues can repress oncogenic transformation. $Arf^{-/-}$ or $Dmp1^{-/-}$ MEFs were infected with lentivirus encoding an empty vector control or Ras^{V12}. $Dmp1^{-/-}$ MEFs were also infected with lentiviruses encoding short hairpin against Arf or the siScramble control, as indicated. (A and B) A total of 1×10^3 cells were seeded in triplicate in medium containing soft agar and were assessed for colony formation 21 days later. (A) Infected cells were lysed, and separated proteins were immunoblotted for indicated proteins. Representative images of colonies are also depicted. (B) Quantification of the number of colonies. Representative data are expressed as the mean ± standard deviation, and P values were calculated using the Student t test. (C) Infected cells were harvested and stained with FITC-annexin V and propidium iodide and subjected to flow cytometry analysis. Representative data are expressed as the mean ± standard deviation of 10,000 events performed in triplicate. (D and E) A total of 2×10^6 cells infected with lentivirus encoding Ras^{V12} were subcutaneously injected into the left flank of athymic nude mice. Five mice were injected per condition, such that each mouse received one injection site. (D) Images of mice and excised tumors are depicted. (E) Tumor diameter was measured in two planes with a digital caliper on successive days postinjection. Tumor volume is expressed as the mean ± standard error of the mean. Excess infected cells from the day of injection were lysed, and separated proteins were immunoblotted for indicated proteins (inset).

knowdown of ARF in $Dmp1^{-/-}$ MEFs restored the tumorigenic potential of these cells, partially phenocopying the tumor burden observed in $Arf^{-/-}$ MEFs infected with Ras^{V12}-encoding virus (Fig. 11D and E). Collectively, these data support the model that ARF acts as a critical checkpoint against hypergrowth stimuli and that in response to these stimuli, ARF can repress cellular transformation (Fig. 12).

DISCUSSION

ARF is a key tumor suppressor responsible for safeguarding the cell against oncogenic stimuli. While it has long been appreciated that ARF can inhibit cell cycle progression, both through p53-dependent and p53-independent mechanisms, the context of stimuli to which ARF responds has predominantly been categorized as hyperproliferative cues. Our results now demonstrate that
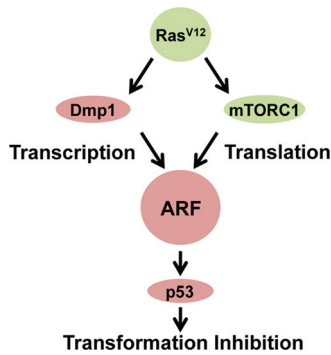
FIG 12 Model. Hypergrowth stimuli emanating from hyperactivation of the mTORC1 pathway induce an ARF checkpoint through a novel translational mechanism. In response to these oncogenic cues, ARF can activate a p53-mediated cell cycle arrest that represses cellular transformation.

ARF has a novel and important role sensing unwarranted hypergrowth stimuli, such as those emanating from robust activation of the mTORC1 signaling pathway. Given that cellular growth and proliferation are in fact two distinct biological processes, albeit highly integrated, we envision a broader range of oncogenic stimuli to which ARF can respond in its antitumorigenic efforts. Since oncogenic stimuli provide the selective pressure for the outgrowth of cancer cells that evade ARF tumor suppression (50), it is important to better understand the array of oncogenic stimuli that are susceptible to ARF tumor surveillance.

In agreement with other groups, we observed that ARF is still capable of responding to Ras^{V12} without transcriptional induction of *Arf* mRNAs by Dmp1. We found that the mTORC1 pathway regulates ARF protein levels through a novel translational mechanism; *Arf* mRNA showed enhanced association with actively translating polyribosomes in response to Ras^{V12} and *Tsc1* loss. ARF induced from *Tsc1* loss facilitated p53 pathway activation and cell cycle arrest. Furthermore, translationally regulated ARF protein repressed anchorage-independent colony formation in soft agar and tumor burden in an allograft model. Therefore, we propose that the cell utilizes this ARF checkpoint as a means to keep excessive progrowth cues under scrutiny.

Of note, *Tsc1*$^{-/-}$ MEFs have been reported to display a lower proliferative rate than *Tsc1*$^{+/-}$ or *Tsc1*$^{+/+}$ MEFs (26). Also, Zhang et al. have shown that primary *Tsc2*$^{-/-}$ MEFs display early senescence in conjunction with a higher expression of p21 (55). Our data suggest that this increase in p21 and the resultant decrease in proliferation could be facilitated in part by the translational ARF induction that ensues from the activation of mTORC1; we observed that p21 induction was abrogated upon the removal of *Arf* in *Tsc1*$^{-/-}$ cells and that loss of *Arf* rescued the proliferation defect observed in cells lacking *Tsc1*.

We envisage collaboration between the Ras/TSC/mTORC1 and the Ras/Dmp1 pathways which together coordinate ARF induction from oncogenic Ras^{V12} overexpression. The involvement of the mTORC1 pathway could explain why Ras^{V12}-mediated ARF induction is compromised, but not completely lost, in a *Dmp1*$^{-/-}$ setting. Given the absolute necessity for cancer cells to bypass ARF's checkpoint against oncogenic stimuli, it is not surprising that multiple regulatory mechanisms would allow ARF to sense as many oncogenic cues as possible.

Deregulation of the members of the mTOR pathway is impli-

cated in the mechanism driving hamartoma-forming diseases. Tuberous sclerosis complex is characterized by the potential for hamartoma formation in a wide spectrum of organs (14). Loss or reduction in function of the TSC1-TSC2 protein complex and the resulting constitutive mTOR signaling are the contributing factors for this disease (6). Our finding that loss of *Tsc1* induces an ARF response could give some insight as to why benign hamartomas, as opposed to more aggressive neoplastic tumors, arise in this disease. It is possible that the ARF growth checkpoint could play a putative role in repressing the proliferation of hamartoma-forming cells, thereby inhibiting their progression to a more aggressive neoplastic tumor; these hypotheses would need to be formally tested. It is of note that analysis of pleomorphic xanthoastrocytoma (PXA), a rare astrocytic tumor in the cerebral hemispheres of children and young adults, was reported to have homozygous deletion of the *CDKN2A/p14*^{Arf} and *CDKN2B* loci as well as reduced *Tsc1* mRNA expression as defining molecular alterations (54). This finding suggests that concomitant loss of *Tsc1* and *Arf* can contribute to the mechanisms driving tumorigenesis.

In the current study, we have described the involvement of the mTORC1 pathway in the regulation of the ARF tumor suppressor via a translational mechanism. It has been readily shown that mTORC1 signaling can induce the selective translation of specific mRNA targets. One such example is the stimulation of p53 translation that occurs upon the loss of *Tsc1* in response to stress conditions (27). It was shown that mTOR can regulate p53 protein synthesis and that hyperactivation of the mTOR pathway can increase sensitivity to DNA damage and energy starvation. In fact, other reports have further elucidated potential mechanisms by which p53 can be translationally regulated (5, 47). Additionally, mTORC1 signaling has been reported to specifically modulate the translation of myeloid cell leukemia sequence 1 (Mcl-1) (32). Loss of *Tsc2* in Eµ-Myc cells increases the translation of Mcl-1, and this modulation of Mcl-1 by mTORC1 is relevant to the chemosensitivity of these tumors. Also, mTORC1 signal transduction modulates the translation of nucleophosmin through a mechanism mediated by FBP1 acting as a regulatory RNA binding protein (33, 35). Here, we show that ARF is another translationally regulated gene product as *Arf* mRNA has enhanced association with actively translating polyribosomes in response to enhanced mTORC1 signal transduction. Translational control of ARF, as well as of these other translationally regulated mRNAs, can serve as a versatile and robust mode of regulation for essential cellular functions.

Further elucidation of the molecular mechanism driving ARF's responsiveness to mTORC1 signaling is of great significance. The implications include the potential identification of novel downstream players not otherwise thought of in the context of the ARF/p53 regulatory network whose interrogation could potentially open avenues to new cancer therapeutics.

REFERENCES

1. **Apicelli AJ, et al.** 2008. A non-tumor suppressor role for basal p19ARF in maintaining nucleolar structure and function. Mol. Cell. Biol. **28:** 1068–1080.

2. **Azzam ME, Algranati ID.** 1973. Mechanism of puromycin action: fate of ribosomes after release of nascent protein chains from polysomes. Proc. Natl. Acad. Sci. U. S. A. **70:**3866–3869.

3. **Bates S, et al.** 1998. p14ARF links the tumour suppressors RB and p53. Nature **395:**124–125.

4. **Brady SN, Yu Y, Maggi LB, Jr, Weber JD.** 2004. ARF impedes NPM/B23 shuttling in an Mdm2-sensitive tumor suppressor pathway. Mol. Cell. Biol. **24:**9327–9338.

5. **Chen J, Kastan MB.** 2010. 5′-3′-UTR interactions regulate p53 mRNA translation and provide a target for modulating p53 induction after DNA damage. Genes Dev. **24:**2146–2156.

6. **Crino PB, Nathanson KL, Henske EP.** 2006. The tuberous sclerosis complex. New Engl. J. Med. **355:**1345–1356.

7. **Dai Y, Grant S.** 2010. New insights into checkpoint kinase 1 in the DNA damage response signaling network. Clin. Cancer Res. **16:**376–383.

8. **de Stanchina E, et al.** 1998. E1A signaling to p53 involves the p19(ARF) tumor suppressor. Genes Dev. **12:**2434–2442.

9. **Elledge SJ.** 1996. Cell cycle checkpoints: preventing an identity crisis. Science **274:**1664–1672.

10. **Grech G, et al.** 2008. Igbp1 is part of a positive feedback loop in stem cell factor-dependent, selective mRNA translation initiation inhibiting erythroid differentiation. Blood **112:**2750–2760.

11. **Guertin DA, Sabatini DM.** 2007. Defining the role of mTOR in cancer. Cancer Cell **12:**9–22.

12. **Hanahan D, Weinberg RA.** 2011. Hallmarks of cancer: the next generation. Cell **144:**646–674.

13. **Hay N, Sonenberg N.** 2004. Upstream and downstream of mTOR. Genes Dev. **18:**1926–1945.

14. **Inoki K, Corradetti MN, Guan KL.** 2005. Dysregulation of the TSC-mTOR pathway in human disease. Nat. Genet. **37:**19–24.

15. **Inoki K, Guan KL.** 2009. Tuberous sclerosis complex, implication from a rare genetic disease to common cancer treatment. Hum. Mol. Genet. **18:** R94–100.

16. **Inoue K, Mallakin A, Frazier DP.** 2007. Dmp1 and tumor suppression. Oncogene **26:**4329–4335.

17. **Inoue K, Roussel MF, Sherr CJ.** 1999. Induction of ARF tumor suppressor gene expression and cell cycle arrest by transcription factor DMP1. Proc. Natl. Acad. Sci. U. S. A. **96:**3993–3998.

18. **Inoue K, et al.** 2000. Disruption of the ARF transcriptional activator DMP1 facilitates cell immortalization, Ras transformation, and tumorigenesis. Genes Dev. **14:**1797–1809.

19. **Inoue K, Zindy F, Randle DH, Rehg JE, Sherr CJ.** 2001. Dmp1 is haplo-insufficient for tumor suppression and modifies the frequencies of Arf and p53 mutations in Myc-induced lymphomas. Genes Dev. **15:** 2934–2939.

20. **Kamijo T, Bodner S, van de Kamp E, Randle DH, Sherr CJ.** 1999. Tumor spectrum in ARF-deficient mice. Cancer Res. **59:**2217–2222.

21. **Kamijo T, et al.** 1997. Tumor suppression at the mouse INK4a locus mediated by the alternative reading frame product p19ARF. Cell **91:** 649–659.

22. **Kastan MB, Bartek J.** 2004. Cell-cycle checkpoints and cancer. Nature **432:**316–323.

23. **Kladney RD, et al.** 2010. Tuberous sclerosis complex 1: an epithelial tumor suppressor essential to prevent spontaneous prostate cancer in aged mice. Cancer Res. **70:**8937–8947.

24. **Knaup KX, et al.** 2009. Mutual regulation of hypoxia-inducible factor and mammalian target of rapamycin as a function of oxygen availability. Mol. Cancer Res. **7:**88–98.

25. **Kuo ML, den Besten W, Bertwistle D, Roussel MF, Sherr CJ.** 2004. N-terminal polyubiquitination and degradation of the Arf tumor suppressor. Genes Dev. **18:**1862–1874.

26. **Kwiatkowski DJ, et al.** 2002. A mouse model of TSC1 reveals sex-dependent lethality from liver hemangiomas, and up-regulation of p70S6 kinase activity in Tsc1 null cells. Hum. Mol. Genet. **11:**525–534.

27. **Lee CH, et al.** 2007. Constitutive mTOR activation in TSC mutants sensitizes cells to energy starvation and genomic damage via p53. EMBO J. **26:**4812–4823.

28. **Livak KJ, Schmittgen TD.** 2001. Analysis of relative gene expression data using real-time quantitative PCR and the $2^{-\Delta\Delta CT}$ method. Methods **25:** 402–408.

29. **Ma XM, Blenis J.** 2009. Molecular mechanisms of mTOR-mediated translational control. Nat. Rev. Mol. Cell Biol. **10:**307–318.

30. Reference deleted.

31. Reference deleted.

32. **Mills JR, et al.** 2008. mTORC1 promotes survival through translational control of Mcl-1. Proc. Natl. Acad. Sci. U. S. A. **105:**10853–10858.

33. **Olanich ME, Moss BL, Piwnica-Worms D, Townsend RR, Weber JD.** 2011. Identification of FUSE-binding protein 1 as a regulatory mRNA-binding protein that represses nucleophosmin translation. Oncogene **30:** 77–86.

34. **Palmero I, Pantoja C, Serrano M.** 1998. p19ARF links the tumour suppressor p53 to Ras. Nature **395:**125–126.

35. **Pelletier CL, et al.** 2007. TSC1 sets the rate of ribosome export and protein synthesis through nucleophosmin translation. Cancer Res. **67:**1609–1617.

36. **Proud CG.** 2007. Signalling to translation: how signal transduction pathways control the protein synthetic machinery. Biochem. J. **403:**217–234.

37. **Quelle DE, Zindy F, Ashmun RA, Sherr CJ.** 1995. Alternative reading frames of the INK4a tumor suppressor gene encode two unrelated proteins capable of inducing cell cycle arrest. Cell **83:**993–1000.

38. **Radfar A, Unnikrishnan I, Lee HW, DePinho RA, Rosenberg N.** 1998. p19(Arf) induces p53-dependent apoptosis during abelson virus-mediated pre-B cell transformation. Proc. Natl. Acad. Sci. U. S. A. **95:** 13194–13199.

39. **Roussel MF, Theodoras AM, Pagano M, Sherr CJ.** 1995. Rescue of defective mitogenic signaling by D-type cyclins. Proc. Natl. Acad. Sci. U. S. A. **92:**6837–6841.

40. **Saporita AJ, Maggi LB Jr, Apicelli AJ, Weber JD.** 2007. Therapeutic targets in the ARF tumor suppressor pathway. Curr. Med. Chem. **14:** 1815–1827.

41. **Shaw RJ, Cantley LC.** 2006. Ras, PI(3)K and mTOR signalling controls tumour cell growth. Nature **441:**424–430.

42. **Sherr CJ.** 2006. Divorcing ARF and p53: an unsettled case. Nat. Rev. Cancer **6:**663–673.

43. **Spriggs KA, Bushell M, Willis AE.** 2010. Translational regulation of gene expression during conditions of cell stress. Mol. Cell **40:**228–237.

44. **Sreeramaneni R, Chaudhry A, McMahon M, Sherr CJ, Inoue K.** 2005. Ras-Raf-Arf signaling critically depends on the Dmp1 transcription factor. Mol. Cell. Biol. **25:**220–232.

45. **Stefani G, Fraser CE, Darnell JC, Darnell RB.** 2004. Fragile X mental retardation protein is associated with translating polyribosomes in neuronal cells. J. Neurosci. **24:**7272–7276.

46. **Strezoska Z, Pestov DG, Lau LF.** 2000. Bop1 is a mouse WD40 repeat nucleolar protein involved in 28S and 5.8S RRNA processing and 60S ribosome biogenesis. Mol. Cell. Biol. **20:**5516–5528.

47. **Takagi M, Absalon MJ, McLure KG, Kastan MB.** 2005. Regulation of p53 translation and induction after DNA damage by ribosomal protein L26 and nucleolin. Cell **123:**49–63.

48. **Tee AR, et al.** 2002. Tuberous sclerosis complex-1 and -2 gene products function together to inhibit mammalian target of rapamycin (mTOR)-mediated downstream signaling. Proc. Natl. Acad. Sci. U. S. A. **99:** 13571–13576.

49. **Thermann R, Hentze MW.** 2007. Drosophila miR2 induces pseudo-polysomes and inhibits translation initiation. Nature **447:**875–878.

50. **Volanakis EJ, Sherr CJ.** 2010. Developmental strategies for evasion of Arf tumor suppression. Cell Cycle **9:**14–15.

51. **Watnick RS, Cheng YN, Rangarajan A, Ince TA, Weinberg RA.** 2003. Ras modulates Myc activity to repress thrombospondin-1 expression and increase tumor angiogenesis. Cancer Cell **3:**219–231.

52. **Weber JD, et al.** 2000. Cooperative signals governing ARF-mdm2 interaction and nucleolar localization of the complex. Mol. Cell. Biol. **20:** 2517–2528.

53. **Weber JD, Taylor LJ, Roussel MF, Sherr CJ, Bar-Sagi D.** 1999. Nucleolar Arf sequesters Mdm2 and activates p53. Nat. Cell Biol. **1:**20–26.

54. **Weber RG, et al.** 2007. Frequent loss of chromosome 9, homozygous CDKN2A/p14(ARF)/CDKN2B deletion and low TSC1 mRNA expression in pleomorphic xanthoastrocytomas. Oncogene **26:**1088–1097.

55. **Zhang H, et al.** 2003. Loss of Tsc1/Tsc2 activates mTOR and disrupts PI3K-Akt signaling through downregulation of PDGFR. J. Clin. Invest. **112:**1223–1233.

56. **Zindy F, et al.** 1998. Myc signaling via the ARF tumor suppressor regulates p53-dependent apoptosis and immortalization. Genes Dev. **12:**2424–2433.

57. **Zoncu R, Efeyan A, Sabatini DM.** 2011. mTOR: from growth signal integration to cancer, diabetes and ageing. Nat. Rev. Mol. Cell Biol. **12:**21–35.